N66-12170
(ACCESSION NUMBER)
118
(PAGES)
CR 68275
(NASA CR OR TMX OR AD NUMBER)
(THRU)
1
(CODE)
14
(CATEGORY)

GPO PRICE $ _____
CFSTI PRICE(S) $ _____
Hard copy (HC) 4.00
Microfiche (MF) .75
ff 653 July 65

LOCKHEED · CALIFORNIA COMPANY
A DIVISION OF LOCKHEED AIRCRAFT CORPORATION

REPORT NO. LR 17491
DATE January 1964
MODEL ---
COPY NO.

TITLE
SOME ASPECTS OF HYPERALTITUDE PHOTOGRAMMETRY

REFERENCE PHOTO INTERPRETATION AND PHOTOGRAMMETRY OF HYPERALTITUDE PHOTOGRAPHY

CONTRACT NUMBER(S) NAS 5-3390

PREPARED BY
R. M. L. Baker Jr., ASTRODYNAMICS

APPROVED BY
Lewis Larmore, CHIEF SCIENTIST

The information disclosed herein was originated by and is the property of the Lockheed Aircraft Corporation, and except for uses expressly granted to the United States Government, Lockheed reserves all patent, proprietary, design, use, sale, manufacturing and reproduction rights thereto. Information contained in this report must not be used for sales promotion or advertising purposes.

REVISIONS

REV. NO.	DATE	REV. BY	PAGES AFFECTED	REMARKS

FORM 402-2

LOCKHEED-CALIFORNIA COMPANY

Division of Lockheed Aircraft Corporation
Burbank, California

SOME ASPECTS OF HYPERALTITUDE PHOTOGRAMMETRY

REPORT NO. 1

CONTRACT NO. NAS 5-3390

Contract Title

PHOTO INTERPRETATION AND PHOTOGRAMMETRY
OF HYPERALTITUDE PHOTOGRAPHY

January 1964

LR 17491

Prepared For
National Aeronautics & Space Administration
Goddard Space Flight Center
Greenbelt, Maryland

Attention: Dr. J. A. O'Keefe, Code 640
Dr. P. D. Lowman, Jr.

LOCKHEED
CALIFORNIA COMPANY

TABLE OF CONTENTS

SECTION I

INTRODUCTION

Requisite to the interpretation of satellite and rocket photos are answers to such questions as, what was the position of the camera in latitude, longitude and altitude at the time of the exposure? What direction was the camera pointing? How may the location of points of interest in the photo be determined, and what are the effects of relief displacement and atmospheric refraction on the position of the images? These and other questions pertinent to the interpretation of hyper-altitude* photos are treated in this report. The analysis of the information content of existing hyperaltitude photos will constitute later reports under this contract.

Problems that involve the orbit and attitude of a satellite, and the relative position of a satellite and the Sun, fall in the realm of astrodynamics. Accordingly, the notation and style of analysis of these problems presented here are consistent with the practices of this branch of science. On the other hand, problems which involve the measurement of photos are treated in the traditions of conventional photogrammetry. The sections of this report that deal with photographic measurements are designed to furnish the interpreter with basic photogrammetric tools required for the reduction of information contained in hyperaltitude photos. This study follows the

---

* As used in this report, hyperaltitude means greater than 50 km.

premise that hyperaltitude photography will be useful in the early stages of the exploration of planetary surfaces, in that it will furnish information about the composition, texture and structure of the surfaces. Therefore, this work deals mainly with photo interpretation rather than cartography, and high precision in measurement is not a principal requirement. Errors of a few percent are allowable. For example, the curvature of the surface being photographed is considered in the photogrammetric calculations, whereas the planetary flattening is not. When appropriate, rough approximations, as well as more accurate photogrammetric methods, are discussed.

The project manager and principal investigator is Dr. Paul M. Merifield. The astrodynamics aspects were analysed by Mr. Pedro Escobal and Mr. Joseph Ball. Contributions regarding attitude sensing problems were made by Dr. Robert Roberson, and the treatment of atmospheric refraction is largely the work of Dr. Kurt Forster. Mr. James Rammelkamp aided in analysing the photogrammetric problems, and Miss Annette Verner was responsible for the programming.

SECTION II

ASTRODYNAMICAL ASPECTS

II-A: GENERAL REMARKS

The astrodynamical phase of this study can be broken down into three separate and independent analyses with a detailed solution appearing as part of the analyses. The three astrodynamical problems are as follows:

1. Given the orbital elements of a photographing satellite, find the subsatellite point in terms of the geographic east longitude (λ_E), the geodetic latitude (φ), and the altitude (H). Supplementary to this problem is the continuous generation of the ground trace of a satellite about an oblate planet.

2. Given λ_E and φ, find the orbital elements in order that the satellite will fly over a particular ground station at a given time, for example, between 1000 and 1400 local sidereal time.

3. Given a set of orbital elements, find the time interval of camera operation that achieves optimum lighting, either for a particular ground station or regardless of the area photographed.

II-B: SUBSATELLITE POINT AND ALTITUDE

The general outline for finding the subsatellite points of a satellite in an orbit is to take the given set of orbital parameters a, e, i, Ω, ω, and T, which completely describe the orbit, and generate the position of the satellite at a specified time t, which in this case is the exposure time. After the satellite position is found, the next step is to transform these subsatellite positions into the geographic east longitude, geodetic latitude and altitude coordinate system.

Proceeding to calculate the subsatellite points, let

$$a,\ e,\ T,\ i,\ \Omega,\ \omega$$

be the given orbital parameters where

- $a \triangleq$ semi-major axis of orbit,
- $e \triangleq$ orbital eccentricity,
- $i \triangleq$ orbital inclination with respect to the Earth's equatorial plane,
- $\Omega \triangleq$ longitude of the ascending node,
- $\omega \triangleq$ argument of perigee, and
- $T \triangleq$ time of perifocal passage.

It should be noticed that the values of the given elements should always be well defined. If for a particular reason they are

not, e.g., $i = 0$, then Ω becomes indeterminate* and cannot be used to describe the orbit. There are other elements that are well defined throughout all of three space, but are not discussed here.

The orientation vectors $\underline{P}$ and $\underline{Q}$ are calculated first (See Figure 2.1):

$$\begin{aligned} P_x &= \cos\omega \cos\Omega - \sin\omega \sin\Omega \cos i \\ P_y &= \cos\omega \sin\Omega + \sin\omega \cos\Omega \cos i \\ P_z &= \sin\omega \sin i \\ Q_x &= -\sin\omega \cos\Omega - \cos\omega \sin\Omega \cos i \\ Q_y &= -\sin\omega \sin\Omega + \cos\omega \cos\Omega \cos i \\ Q_z &= \cos\omega \sin i \end{aligned} \tag{2.1}$$

Next we define relationships that are needed to express $\underline{r}$ as a function of known quantities where we are considering only elliptical orbits, in which case the mean motion, n, is given by

$$n = k\sqrt{\frac{\mu}{a^3}} , \tag{2.2}$$

where

k = gravitational constant,

μ = mass of central body plus mass of satellite,

and

$$M = n(t - T) , \tag{2.3}$$

---

* The indeterminate elements should then be set by definition, e.g., $\Omega \triangleq 0$, if $i = 0$.

LOCKHEED
CALIFORNIA COMPANY

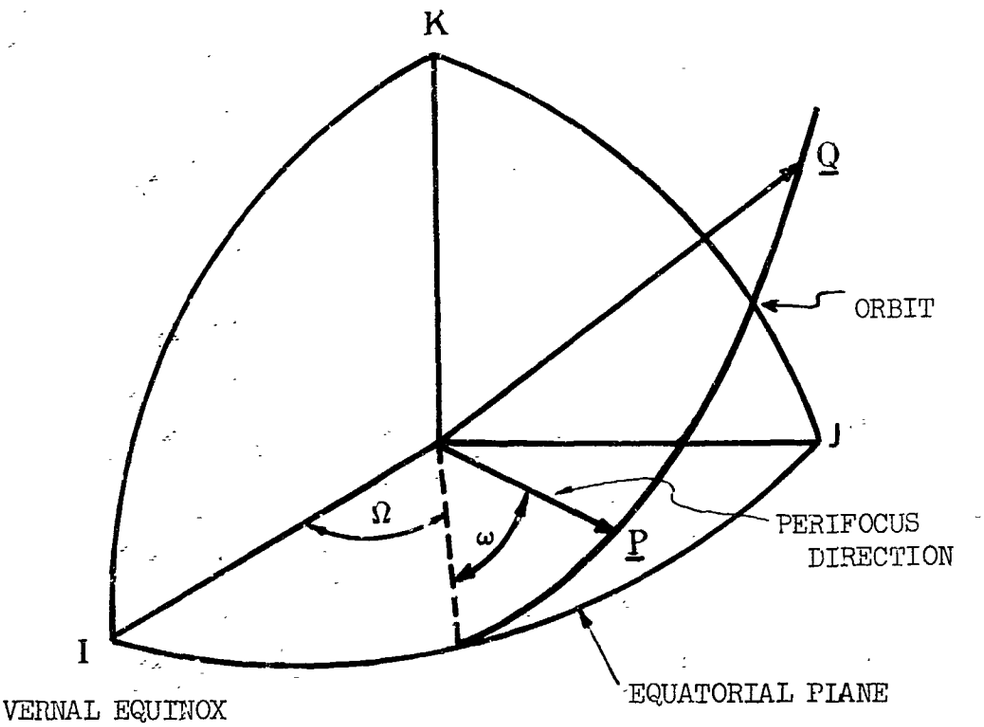

Figure 2.1: Vectors $\underline{P}$ and $\underline{Q}$

with

M = mean anomaly

t = time of photographic exposure in conventional terrestrial units (e.g., hours, minutes, and seconds).

Also

$$M = E - e \sin E, \longrightarrow E^{*} \tag{2.4}$$

where E is the eccentric anomaly.

and

$$x_{\omega} = a(\cos E - e) \tag{2.5}$$

$$y_{\omega} = a\sqrt{1 - e^2} \sin E \tag{2.6}$$

where x_{ω} and y_{ω} are defined in Figure 2.2.

We can now define $\underline{r}$ and $\dot{\underline{r}}$ in terms of known quantities,

$$\underline{r} = x_{\omega}\,\underline{P} + y_{\omega}\,\underline{Q} \tag{2.7}$$

in which $\underline{r}$ is the position vector in the geocentric equatorial coordinate system.

$$r = (\underline{r} \cdot \underline{r})^{\frac{1}{2}} \tag{2.8}$$

$$\dot{x}_{\omega} = -\frac{\sqrt{\mu a}}{r} \sin E \tag{2.9}$$

---

* The symbol $\longrightarrow$ means "yields".

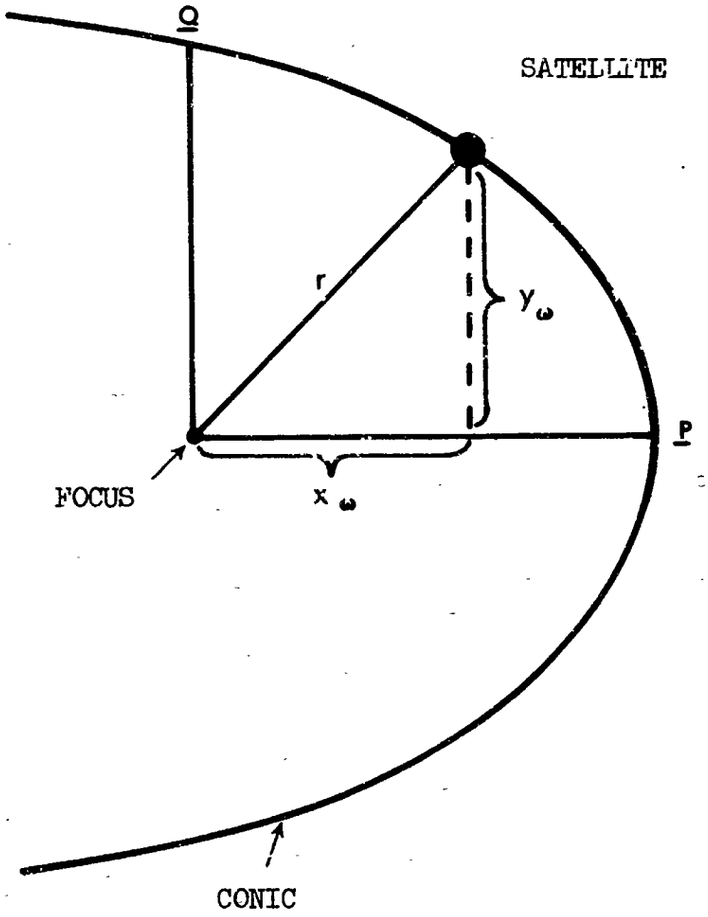

Figure 2.2: Definition of X_ω and Y_ω

$$\dot{y}_\omega = \left[\frac{\sqrt{\mu a(1 - e^2)}}{r} \right] \cos E \tag{2.10}$$

$$\dot{\underline{r}} = \dot{x}_\omega \underline{P} + \dot{y}_\omega \underline{Q} \tag{2.11}$$

in which $\dot{\underline{r}}$ is the velocity vector in the same geocentric equatorial coordinate system.

Since the coordinates of the subsatellite points are in the geocentric equatorial coordinate system, they must be transformed into the geographic coordinate system (λ and φ). This transformation is accomplished as follows:

Symbolically, the transformation is written as

$$x, y, z, t \longrightarrow \varphi_s', \varphi_s, \lambda_E, H_s$$

where

φ_s' = geocentric latitude subvehicle point,

φ_s = geodetic latitude subvehicle point,

λ_E = East longitude measured counterclockwise from the foot of Greenwich meridian, and

H_s = normal altitude of vehicle above reference ellipsoid.

We calculate the radius, r, from

$$r = + \sqrt{x^2 + y^2 + z^2} \tag{2.12}$$

and the right ascension, α, from

$$\alpha = \tan^{-1}\left(\frac{y}{x}\right) \qquad 0^\circ \le \alpha \le 360^\circ \tag{2.13}$$

(examination of the sign of x and y allows quadrant definition). The east longitude, λ_E, can be written as

$$\lambda_E = 360^\circ - \left[\theta_g + \dot{\vartheta}(t - t_o) - \alpha\right] \tag{2.14}$$

$$0^\circ \le \lambda_E \le 360^\circ$$

where θ_g is the sidereal time of Greenwich. Finally, the declination, δ, is obtained from

$$\delta = \tan^{-1}\left[\frac{z}{\sqrt{x^2 + y^2}}\right] \quad . \quad -90^\circ \le \delta \le +90^\circ. \tag{2.15}$$

At this point, unless f (the flattening) is zero, one assumes that $\varphi_s' = \delta$ and continues calculating as follows:

$$r_c = a_e\sqrt{\frac{1 - (2f - f^2)}{1 - (2f - f^2)\cos^2\varphi_s'}} \tag{2.16}$$

where r_c is the geocentric distance of the station,

$$\varphi_s = \tan^{-1}\left[\frac{1}{(1 - f)^2}\ \tan\varphi_s'\right] \tag{2.17}$$

$$-90^\circ \le \varphi_s \le 90^\circ$$

$$H_s = \sqrt{r^2 - r_c^2 \sin^2(\varphi_s - \varphi_s')} - r_c \cos(\varphi_s - \varphi_s') \quad (2.18)$$

$$\Delta\varphi_s' = \sin^{-1}\left[\frac{H_s}{r} \sin(\varphi_s - \varphi_s')\right] . \quad (2.19)$$

Next one recalculates

$$\varphi_s' = \delta - \Delta\varphi_s' \quad (2.20)$$

and returns to Eq. (2.16), repeating this loop until φ_s' is within the desired tolerance.

The ground trace can now be generated from a further extension of the previous procedure by repeating the cycle from Eq. (2.3) to Eq. (2.20) with t or E as the independent variable.*

If the satellite has been in orbit around the Earth at least one revolution and secular correction owing to oblateness of the Earth needs to be included, the orbital elements are corrected and the ground trace generated as follows:

$$\Delta t = t_s - T \quad (2.21)$$

where t_s is the start time. The anomalistic period, P, is given by

$$P = \frac{2\pi}{k_e\sqrt{\mu}} a^{3/2}\left[1 - \frac{3}{2} J_2 \left(\frac{a_e}{a(1-e^2)}\right)^2 \left(1 - \frac{3}{2}\sin^2 i\right)\left(1 - \frac{1}{2} e^2\right)\right] . \quad (2.22)$$

The starting revolution number (N) can be computed by

---

* The ground trace problem appears also in Reference No. 3.

$$N = \text{INTF}\left(\quad \text{(see footnote)} \right) \tag{2.23}$$

$$E - e \sin E = M = \text{M}\phi\text{DF}\left(\frac{2\pi}{P}\, 1440\Delta t,\ 360^{\circ}\right) \longrightarrow E \tag{2.24}$$

(see footnote)

The orbital elements ω and Ω are updated by

$$\omega_N = \omega + \frac{3}{4} J_2 \left(\frac{a_e}{a(1-e^2)}\right)^2 k\sqrt{\mu}\ a^{-3/2} (4 - 5 \sin^2 i)NP \tag{2.25}$$

$$\Omega_N = \Omega - \frac{3}{2} J_2 \left(\frac{a_e}{a(1-e^2)}\right)^2 k\sqrt{\mu}\ a^{-3/2} (\cos i)NP \tag{2.26}$$

One computes and saves

$$M' \triangleq \frac{3}{2} J_2 \left(\frac{a_e}{a(1 - e^2)}\right)^2 \sqrt{\mu(1 - e^2)}\ a^{-3/2} \left(1 - \frac{3}{2} \sin^2 i\right) \tag{2.27}$$

$$\begin{aligned}
P_x &= \cos \omega_N \cos \Omega_N - \sin \omega_N \sin \Omega_N \cos i \\
P_y &= \cos \omega_N \sin \Omega_N + \sin \omega_N \cos \Omega_N \cos i \\
P_z &= \sin \omega_N \sin i \\
Q_x &= -\sin \omega_N \cos \Omega_N - \cos \omega_N \sin \Omega_N \cos i \\
Q_y &= -\sin \omega_N \sin \Omega_N + \cos \omega_N \cos \Omega_N \cos i \\
Q_z &= \cos \omega_N \sin i
\end{aligned} \tag{2.28}$$

$$x_\omega = a(\cos E - e) \tag{2.29}$$

$$y_\omega = a\sqrt{1 - e^2}\ \sin E \tag{2.30}$$

---

* INTF and MΦDF are the standard FORTRAN functions, Integer Function and Mode Function.

$$x = x_\omega P_x + y_\omega Q_x \tag{2.31}$$

$$y = x_\omega P_y + y_\omega Q_y \tag{2.32}$$

$$z = x_\omega P_z + y_\omega Q_z \tag{2.33}$$

$$r = a(1 - e \cos E) \tag{2.34}$$

$$\bar{t} = \left(\frac{1}{k}\right) \frac{(E - e \sin E)}{\sqrt{\mu}\ a^{-3/2} + M'} \tag{2.35}$$

$$\sin \alpha = \frac{y}{\sqrt{x^2 + y^2}} \qquad 0^\circ \le \alpha \le 360^\circ \tag{2.36}$$

$$\cos \alpha = \frac{x}{\sqrt{x^2 + y^2}} \tag{2.37}$$

$$\lambda_E' = \alpha - \theta_g - \dot{\theta} t \tag{2.38}$$

where t is the total number of minutes elapsed since the year, month, and day of t_s, and

$$\lambda_E = M\Phi DF(\lambda_E', 360^\circ) \qquad 0^\circ \le \lambda_E \le 360^\circ \ , \tag{2.39}$$

which is the east longitude of the ground trace. If the flattening $f = 0$, then one sets $\varphi = \delta$ and proceeds to Eq. (2.44); if $f \neq 0$, as a trial, one sets $\varphi_s' = \delta$ and continues calculating with

$$r_c = a_e \left[\frac{1 - (2f - f^2)}{1 - (2f - f^2)\cos^2 \varphi_s'}\right]^{\frac{1}{2}} \tag{2.40}$$

$$\varphi_s = \tan^{-1}\left[\frac{1}{(1-f)^2}\tan\varphi_s'\right] \qquad (2.41)$$

$$-90^\circ \le \varphi_s \le 90^\circ$$

$$H_s = \left[r^2 - r_c^2 \sin^2(\varphi_s - \varphi_s')\right]^{\frac{1}{2}} - r_c\cos(\varphi_s - \varphi_s') \qquad (2.42)$$

$$\Delta\varphi_s' = \sin^{-1}\left[\frac{H_s}{r}\sin(\varphi_s - \varphi_s')\right] \qquad (2.43)$$

$$-90^\circ \le \Delta\varphi_s' \le 90^\circ$$

Next one recalculates

$$\varphi_s' = \delta - \Delta\varphi_s'$$

and returns to Eq. (2.40). This loop is repeated until φ_s' no longer varies. The process at the same time yields the geodetic ground trace latitude.

One checks to see if

$$\nabla = t - t_{sp} > 0 \qquad (2.44)$$

where t_{sp} is the "stop time." If $\nabla > 0$, the machine program "exits"; if not, it checks to see if $E = 360^\circ - \epsilon$ (where ϵ is just to indicate that $\bar{t}$ is equal to the period and not 0). If $E = 360 - \epsilon$, it computes

$$\omega_{N+1} = \omega_N + \frac{3}{4} J_2 \left(\frac{a_e}{a(1-e^2)}\right)^2 k\sqrt{\mu}\, a^{-3/2}\,(4 - 5\sin^2 i)\,\bar{t} \qquad (2.45)$$

LOCKHEED
CALIFORNIA COMPANY

$$\Omega_{N+1} = \Omega_N - \frac{3}{2} J_2 \left(\frac{a_e}{a(1 - e^2)} \right)^2 \left(k\sqrt{\mu} \; a^{-3/2} \cos i \right) \bar{t} \qquad (2.46)$$

and recalculates $\underline{P}$ and $\underline{Q}$ from Eq. (2.28). If $E \neq 360^\circ$, it increments E by

$$E = E + \Delta E$$

and returns to Eq. (2.29).

Once λ_E and φ are determined, they can be plotted on a map to obtain the corresponding ground trace of a satellite in orbit.

II-C: STATION FLY-OVER*

The solution to problem 2, given λ and φ of a ground station to be photographed, determines the orbital elements in order that the satellite will fly over a particular ground station at a given time where, for example, the time is between 1000 and 1400 local sideral time.

The criterion for solving this problem is stated as follows: a satellite is said to have overflown the target where the target is defined as the specified ground station at some time t, if the magnitude of the normal from the orbit plane that intersects the station is identically zero.

From the previous criterion, it is possible to proceed as follows. Introduce the right handed set of unit vectors $\underline{P}$, $\underline{Q}$ and $\underline{W}$ into the right ascension-declination coordinate system such that $\underline{P}$ and $\underline{Q}$ define the orientation plane of the desired orbit plane. $\underline{P}$ is taken in the perifocal direction, and $\underline{Q}$ is advanced by a right angle to $\underline{P}$ in the direction of motion; $\underline{W}$ is taken normal to the orbit plane.

Examination of Figure 2.3 permits the following vector equation to be written.

$$\underline{R} + \underline{T} + \underline{A} = 0 \qquad (2.47)$$

---

* Appears also in Reference No. 2.

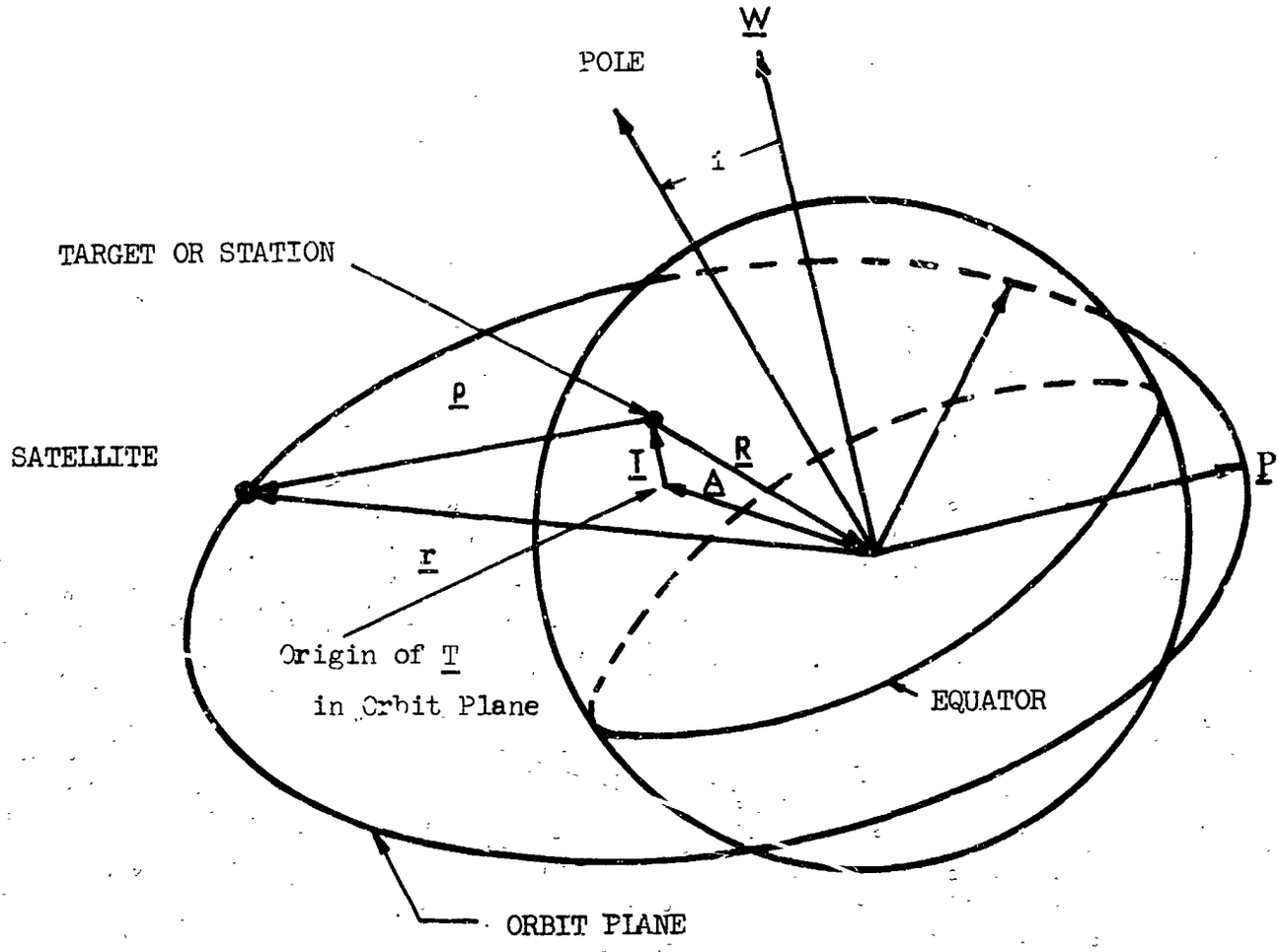

Figure 2.3
Orbit Geometry

LOCKHEED
CALIFORNIA COMPANY

where

$\underline{R}$ = a vector from the specified target station to the dynamical center;

$\underline{T}$ = a vector normal to the orbit plane that terminates at target station;

$\underline{A}$ = a vector from the dynamical center to the origin $\underline{T}$ in the unknown orbit plane.

By dotting Eq. (2.47) with $\underline{W}$ it is possible to write

$$\underline{W}\cdot\underline{R} + \underline{W}\cdot\underline{A} + \underline{W}\cdot\underline{T} = 0 \tag{2.48}$$

but

$$\underline{W}\cdot\underline{A} = 0 \tag{2.49}$$

since $\underline{W}$ is perpendicular to $\underline{A}$ and

$$\underline{W}\cdot\underline{T} = T \tag{2.50}$$

where $\underline{W}$ is a unit vector parallel to $\underline{T}$ and the angle between $\underline{W}$ and $\underline{T}$ is zero. Therefore, Eq. (2.48) states that

$$T = -\underline{W}\cdot\underline{R} \quad . \tag{2.51}$$

Before evaluating Eq. (2.51), a slight digression into the station coordinates of the target station is required. In terms of the geodetic latitude φ and the local sidereal time θ, where

$$\theta = \theta_g + .004,375,269,50(t - t_o) + \lambda_E$$

$(t - t_o)$ = the solar time in minutes since the epoch,

the components of the station radius vector $\underline{R}$ for an oblate spheriod are given by

$$\left.\begin{aligned} X &= - G_1 \cos\varphi \cos\theta \\ Y &= - G_1 \cos\varphi \sin\theta \\ Z &= - G_2 \sin\varphi \end{aligned}\right\} \quad (2.52)$$

where

$$G_1 \triangleq \frac{a_e}{\sqrt{1 - (2f - f^2)\sin^2\varphi}} + H \triangleq C + H$$

$$G_2 \triangleq \frac{a_e(1 - f)^2}{\sqrt{1 - (2f - f^2)\sin^2\varphi}} + H \triangleq S + H$$

and

a_e = equatorial radius of planet,

f = flattening of adopted ellipsoid,

H = station elevation above and measured normal to the surface of the adopted ellipsoid, and

θ = local sidereal time.

Therefore, by evaluating the dot product defined by Eq. (2.51), it is possible to express the constraining equation as

$$T = -(W_x X + W_y Y + W_z Z) \tag{2.53}$$

or more exactly as

$$T = G_1 W_x \cos\varphi \cos\theta + G_1 W_y \cos\varphi \sin\theta + G_2 W_z \sin\varphi \quad . \tag{2.54}$$

Equation (2.54) is the sought for constraint.

Solution of the Constraining Equation

It is obvious that if T is set equal to zero, a relationship will exist between W_x, W_y, and W_z such that the station or target will be in the plane of the orbit. Furthermore, the components of the $\underline{W}$ vector are related by means of

$$W_x^2 + W_y^2 + W_z^2 = 1 \quad . \tag{2.55}$$

Hence, simultaneous solution of Eqs. (2.54) and (2.55) with T set equal to zero will solve the orientation part of the fly-over problem. However, for most applications, i.e., photogrammetry, etc. it will also be beneficial to make the rate of change the scalar T (the normal to the orbit plane) with respect to θ (the sidereal time) at the fly-over point zero. Naturally, this will result in a better

photograph of the target site.* Therefore, from Eq. (2.54)

$$\frac{dT}{d\theta} = - G_1 W_x \cos \varphi \sin \theta + G_1 W_y \cos \varphi \cos \theta \qquad (2.56)$$

and

$$\frac{d^2T}{d\theta^2} = - G_1 W_x \cos \varphi \cos \theta - G_1 W_y \cos \varphi \cos \theta \qquad (2.56)$$

So that from Eq. (2.56) setting $dT/d\theta = 0$,

$$-W_x \sin \theta + W_y \cos \theta = 0 \qquad (2.58)$$

or

$$\tan \theta = \frac{W_y}{W_x} \quad , \qquad (2.59)$$

---

* Evidently there is a conflict between a speed constraint, i.e., slowest speed over the station and a height constraint. Therefore, if the speed of the satellite is decreased, the height will be increased. These are dynamical constraints and will not be discussed at this point. In passing, it is well to note that there are an infinite number of orbits with $\underline{T} = 0$.

However, it certainly appears feasible to have the normal component $(dT/d\theta)$ of station velocity equal to zero by proper choice of elements. Furthermore, since

$$R^2 = A^2 + T^2$$

or by differentiation,

$$A \frac{dA}{d\theta} + T \frac{dT}{d\theta} = 0$$

a value of $dT/d\theta = 0$ implies that $dA/d\theta$ is zero (the radial rate). Therefore, the velocity vectors of the satellite and station will be co-planer. In effect the satellite will then be "panning" the scene.

It must be remembered that W_x and W_y must be chosen such that

$$\frac{d^2T}{d\theta^2} = - G_1 \cos\varphi \left[W_x \cos\theta + W_y \sin\theta \right] > 0 \qquad (2.60)$$

in order to insure a minimum value for the magnitude of T as the fly-over point.

Substituting Eqs. (2.55) and (2.59) into Eq. (2.54) results in

$$G_1 W_x \cos\varphi \cos\theta + G_1 W_x \cos\varphi \tan\theta \sin\theta \pm G_2 \sin\varphi \left[1 - W_x^2 - W_x^2 \tan^2\theta \right]^{\frac{1}{2}} = 0 \qquad (2.61)$$

or

$$\frac{G_1 W_x \cos\varphi}{\cos\theta} \pm G_2 \sin\varphi \left(1 - W_x^2 \sec^2\theta \right)^{\frac{1}{2}} = 0 \quad . \qquad (2.62)$$

By transposing, squaring both sides, and collecting terms, the W_x component of the $\underline{W}$ vector is therefore found to be

$$W_x = \pm \frac{G_2 \sin\varphi \cos\theta}{G_o} \qquad (2.63)$$

with

$$G_o^2 = G_2^2 \sin^2\varphi + G_1^2 \cos^2\varphi \quad . \qquad (2.64)$$

Then from Eq. (2.59)

$$W_y = \pm \frac{G_2 \sin\varphi \sin\theta}{G_o} \qquad (2.65)$$

Finally Eq. (2.55) yields

$$W_z = \pm \frac{\sqrt{G_o^2 - G_2^2 \sin^2\varphi}}{G_o} \quad . \tag{2.66}$$

In order to insure a minimum value for the magnitude of T it is possible to show that W_x and W_y take the lower signs if a station is above the equator and the upper signs if a station is below the equator. This can be seen by substitution of Eqs. (2.63) and (2.65) into Eq. (2.60). Hence

$$\frac{d^2T}{d\theta^2} = -\frac{1}{2}\frac{G_1 G_2}{G_o} \sin 2\varphi \left[\pm \cos^2\theta \pm \sin^2\theta\right] \quad , \tag{2.67}$$

so that if $\varphi > 0$, taking the lower sign

$$\frac{d^2T}{d\theta^2} = \frac{1}{2}\frac{G_1 G_2}{G_o} \sin 2\varphi > 0 \quad ,$$

and likewise if $\varphi < 0$, taking the upper sign

$$\frac{d^2T}{d\theta^2} = -\frac{1}{2}\frac{G_1 G_2}{G_o} \sin 2\varphi > 0 \quad .$$

The sign of W_z is taken as desired, since both retrograde ($W_z < 0$) and direct orbits ($W_z > 0$) can be used to solve the fly-over problem.*

---

* A retrograde orbit will destroy the 'panning' effect discussed in footnote on page 23.

Equations (2.63), (2.65), and (2.66) can be conveniently rewritten as

$$\left.\begin{aligned} W_x &= \pm \frac{G_2}{G_o} \sin\varphi \cos\left[\theta_e + \dot{\theta}(t - t_e)\right] \\ W_y &= \pm \frac{G_2}{G_o} \sin\varphi \sin\left[\theta_e + \dot{\theta}(t - t_e)\right] \\ W_z &= \pm \frac{1}{G_o} \sqrt{G_o^2 - G_2^2 \sin^2\varphi} \end{aligned}\right\} \quad (2.68)$$

which, as shall be presently shown, in effect completely solves the orientation problem with due regard for the sign of each quantity as indicated previously; and where

t = desired station universal fly-over time,

t_e = station universal time at epoch,

$\dot{\theta}$ = sidereal rate of change = constant, and

θ_e = station sidereal time at epoch.

The unit vector $\underline{W}$ is related to the classical orientation angles by means of

$$\begin{aligned} W_x &= \sin\Omega \sin i \qquad 0 \le \Omega \le 2\pi \\ W_y &= -\cos\Omega \sin i \qquad 0 \le i \le \pi \\ W_z &= \cos i \end{aligned} \quad (2.69)$$

so that

LOCKHEED
CALIFORNIA COMPANY

$$\left.\begin{aligned} \sin i &= + \sqrt{1 - W_z^2} \\ \cos i &= W_z \end{aligned}\right\} \longrightarrow i$$

$$\left.\begin{aligned} \sin \Omega &= \frac{W_x}{\sin i} \\ \cos \Omega &= - \frac{W_y}{\sin i} \end{aligned}\right\} \longrightarrow \Omega \quad . \tag{2.70}$$

This completely determines i, the orbital inclination and Ω, the longitude of the ascending node. From the analysis, it is evident that only these two angles are needed to solve the fly-over problem. Therefore ω, the argument of perigee, which is the third orientation element of the classical set

$$i, \Omega, \omega$$

can be picked as desired. Having picked ω, it is possible to calculate the vectors $\underline{P}$ and $\underline{Q}$, where $\underline{Q}$ is a unit vector advanced to $\underline{P}$ by a right angle in the plane of motion as follows:*

$$\begin{aligned} P_x &= \cos \omega \cos \Omega - \sin \omega \sin \Omega \cos i \\ P_y &= \cos \omega \sin \Omega + \sin \omega \cos \Omega \cos i \\ P_z &= \sin \omega \sin i \\ Q_x &= -\sin \omega \cos \Omega - \cos \omega \sin \Omega \cos i \\ Q_y &= -\sin \omega \sin \Omega + \cos \omega \cos \Omega \cos i \\ Q_z &= \cos \omega \sin i \quad . \end{aligned} \tag{2.71}$$

---

* Advantage can be taken by choosing $\omega = 0$ because the calculation of $\underline{P}$ simplifies greatly. $\underline{Q}$ can always be obtained from $\underline{Q} = \underline{W} \times \underline{P}$. These vectors are calculated here because they will be used in the next section.

The Dimensional Elements

In the previous section the orientation elements i, Ω, and ω have been determined such that the station or target is in the plane of the orbit at the desired time t. The dimensional elements i.e.,

$$a,\ e,\ T_P$$

where

a = semimajor axis

e = orbital eccentricity

T_P = time of perifocal passage

are still undetermined. Actually no explicit relationship is imposed upon these elements in the orientation solution of the fly-over problem. However, a useful extension to the fly-over problem is of course the condition that the satellite, which is now in a predetermined plane, shall be directly over the station at a specified time and at a specified altitude H_c.*

To be more specific, if the altitude of the satellite (above and measured normal to the surface of the adopted ellipsoid) is a given constraint, which is to be in effect at time t, it is possible to compute the magnitude of the radius vector at t by

$$r = \sqrt{r_c^2 + H_s^2 + 2r_c H_s \cos(\varphi_s - \varphi_s')} \quad , \qquad (2.72)$$

* The subscript s refers to subvehicle point.

where the geocentric latitude φ' of the station is obtained as a function of the flattening f by

$$\varphi_s' = \tan^{-1}\left[(1 - f)^2 \tan \varphi\right] \qquad -90^\circ \leq \varphi_s' \leq 90^\circ \tag{2.73}$$

and the distance from the dynamical center to the ellipsoid, r_c, is given by

$$r_c^2 = \frac{a_e^2\left[1 - (2f - f^2)\right]}{1 - (2f - f^2)\cos^2\varphi_s'} \quad . \tag{2.74}$$

Hence, given H_s, it is certainly possible to compute the magnitude of the radius vector r to the satellite.

The true anomaly v of the satellite can be directly calculated if it is realized that at the fly-over point the station radius vector is in the plane of the orbit. Therefore, by defining the unit vector $\underline{U}$ as

$$\underline{U} = -\frac{\underline{R}}{R} \quad , \tag{2.75}$$

i.e., a unit vector pointing directly to the satellite at the fly-over point, it follows that

$$\cos v = \underline{U} \cdot \underline{P} \tag{2.76}$$

and

$$\sin v = -(\underline{U} \times \underline{P}) \cdot \underline{W} \tag{2.77}$$

It should be noticed that $\underline{P}$ is defined by means of Eqs. (2.71) and that only one component of Eq. (2.77) is needed.*

Now since no further conditions are imposed upon the specific orbit, e.g., minimum time to the station from a given position in the orbit etc., it is possible to arbitrarily pick a dimensional element; let it be e, the eccentricity. By means of the mapping

$$\cos E = \frac{\cos v + e}{1 + e \cos v}$$
$$\sin E = \frac{\sqrt{1 - e^2}\ \sin v}{1 + e \cos v} \qquad (2.78)$$

the eccentric anomaly E is readily computed and thus the semi-major axis of the orbit, a, is

$$a = \frac{r}{1 - e \cos E} \quad . \qquad (2.79)$$

Then utilizing Kepler's equation in the form

$$T_p = t - \left[\frac{E - e \sin E}{k\sqrt{\mu}}\right] a^{3/2} \qquad (2.80)$$

where**

k = gravitational constant of the planet

μ = sum of the masses of the two bodies

---

* Obviously the largest component of $\underline{W}$ should be used to yield the greatest accuracy.

** The time, t, in Eq.(2.80) should be the universal time. However, if this is understood it suffices to use t in minutes measured from t_e.

allows for the determination of the time of perifocal passage, T_p.

This satellite, with elements of orientation i and Ω, from Eqs. (2.69) and an arbitrary value of ω; along with the dimensional element a from Eq. (2.79) the T_p obtained from Eq. (2.80) with arbitrary e, will be directly over the station or target at time t with altitude H_s.

Solution with a Fixed Orbital Inclination

Since the constraint of a fixed inclination is quite strong, a solution to this problem is presented for the sake of completeness.

It follows that if i is specified then Eq. (2.55) yields

$$W_x^2 + W_y^2 = 1 - \cos^2 i = 1 - W_{zo}^2 \qquad (2.81)$$

where the zero subscript means that W_z is held constant. The condition $T = 0$ produces the following relation from Eq. (2.54)

$$G_1 W_x \cos\varphi \cos\theta + G_1 W_y \cos\varphi \sin\theta = - G_2 W_{zo} \sin\varphi \ . \qquad (2.82)$$

This in effect is the solution of the problem, for W_x and W_y are determined as the solutions of the intersection of a straight line, Eq. (2.82) and a circle, Eq. (2.81). Substitution of W_y from Eq. (2.82) into Eq. (2.81) produces the quadratic in W_x.

LOCKHEED
CALIFORNIA COMPANY

$$W_x^2 + 2\left[\left(\frac{G_2}{G_1}\right) W_{zo} \tan\varphi \cos\theta\right] W_x + \left[\left(\frac{G_2}{G_1}\right)^2 W_{zo}^2 \tan^2\varphi - (1 - W_{zo}^2)\sin^2\theta\right] = 0 \quad . \tag{2.83}$$

Hence, after obtaining a root of Eq. (2.83), W_y is obtained from the linear contraint i.e., Eq. (2.82). The solution then continues as indicated previously, starting with Eqs. (2.70).

A set of expressions have been developed that enable the orientation elements of an orbit to be determined such that on any day at a given local time, a specified ground station will be in the plane of the orbit.* The chosen local time, when converted to universal time is the t for Eqs. (2.68); furthermore, the lateral rate of change of the station out of the orbit plane is taken to be zero in order to obtain a smoother passage. As an added extension, a technique has been developed that will place the satellite at a specified height above the desired station or target at the specified time. Solution of the complete fly-over problem as developed here requires that two elements of the orbit be arbitrarily chosen to best suit the problem at hand. The other four are defined by choosing the desired t and evaluating the respective equations.

---

* The most effective photographing times are 1000 and 1400 local time over a particular station (except for ground observation north of the Arctic circle and south of the Antarctic circle). However, useful photography can be obtained during the time interval 1000-1400 hours. Within the Arctic and Antarctic circles, the photographing time t for use in Eqs. (2.68), becomes more restrictive; i.e., the days of the year along with the time of day must be considered when fixing the orbital elements of a satellite.

A solution with a fixed inclination has also been developed. Since the solution is achieved in closed form, a great saving in machine time will be realized.

SECTION II-D: OPTIMUM ILLUMINATION FOR PHOTOGRAPHY

Consider the third problem of obtaining specific viewing times when a satellite can photograph a given ground station that must be bathed in direct sunlight.

From Figure 2.4, the constraining geometry of the problem demands that

$$-\underline{R}_\odot \cdot \underline{R} = R_\odot R \cos (< \underline{R}_\odot, -\underline{R}) . \qquad (2.84)$$

The vector $\underline{R}_\odot$ is the Sun's radius vector in the geocentric equatorial coordinate system. The components are tabulated in the American Ephemeris and Nautical Almanac at convenient intervals. This vector has the components $X_\odot$, $Y_\odot$, $Z_\odot$.

The station or desired photographic point is located by the vector $\underline{R}$, with components X, Y, Z, defined by

$$\left.\begin{aligned} X &= -G_1 \cos\varphi \cos\theta \\ Y &= -G_1 \cos\varphi \sin\theta \\ Z &= -G_2 \sin\varphi \end{aligned}\right\} \quad (2.85)$$

What is now needed is a criteria for deciding at what times it will be best to photograph a particular spot on the Earth's surface. If one arbitrarily defines a particular angle between the magnitudes of the $\underline{R}$ and $\underline{R}_\odot$ vectors by ψ, then as can be seen from Fig. 2.5, selecting a ψ less than $\pi/2$ will have the result of assuming that sunlight

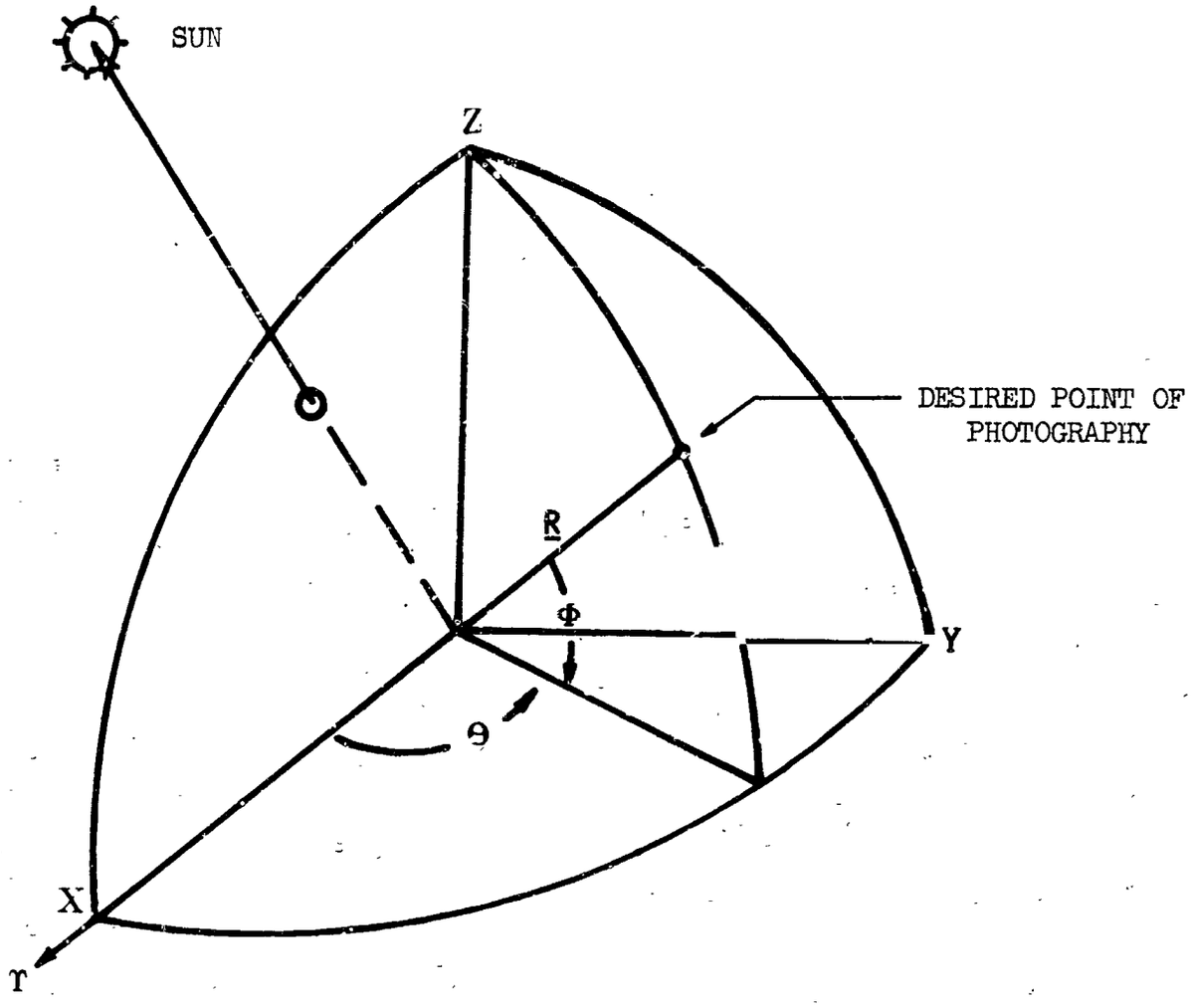

Figure 2.4: Sun-Earth System

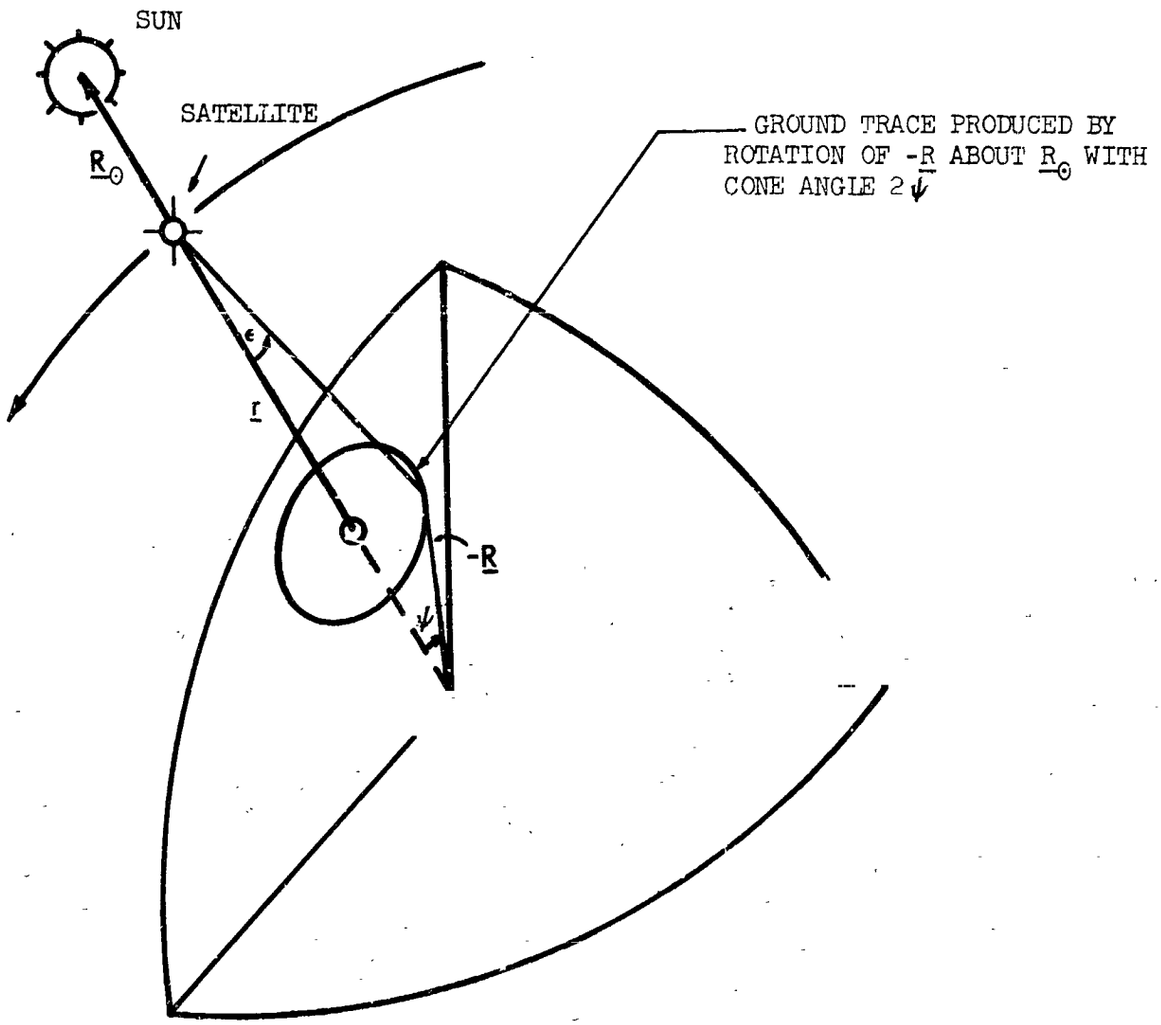

Figure 2.5: Illumination Geometry

exists over the desired point of photography. Furthermore, if $\psi = 0$, then this would have the effect of placing the Sun directly over the station, etc. Hence, picking any ψ less than $\pi/2$ will result in an elliptical ground trace or slight oval which always will be bathed in nearly direct sunlight. It should be noticed that ψ may very will be set by ϵ (see Fig. 2.5), i.e., the half cone angle ϵ of the satellites camera field of view. This is a function of the total angular spread of the photographic lens and the satellite orbit.*

At any rate, Eq. (2.8[illegible] may be written as

$$-\frac{\underline{R}_\odot}{R_\odot} \cdot \frac{\underline{R}}{R} = \cos\psi \quad , \tag{2.86}$$

which upon expansion becomes

$$\frac{X_\odot}{RR_\odot} G_1 \cos\varphi \cos\theta + \frac{Y_\odot}{RR_\odot} G_1 \cos\varphi \sin\theta + \frac{Z_\odot}{RR_\odot} G_2 \sin\varphi = \cos\psi \quad . \tag{2.87}$$

We define the following readily computable coefficients:

$$\alpha \triangleq \frac{X_\odot G_1}{RR_\odot} \cos\varphi$$

$$\beta \triangleq \frac{Y_\odot}{RR_\odot} G_1 \cos\varphi$$

---

* $\psi = \sin^{-1}\left[\frac{H}{R}\tan\epsilon\right]$, $0 \le \psi \le \frac{\pi}{2}$, where H is the satellite altitude above the surface of the Earth.

and

$$\gamma \triangleq \frac{Z_\odot}{RR_\odot} G_2 \sin \varphi \quad , \tag{2.89}$$

and Eq. (2.87) reduces to

$$\alpha \cos \theta + \beta \sin \theta = \cos \psi - \gamma \quad . \tag{2.89}$$

Furthermore, by dividing both sides of Eq. (2.89) by $+\sqrt{\alpha^2 + \beta^2}$ and realizing that by definition

$$\cos \zeta \triangleq \frac{\alpha}{\sqrt{\alpha^2 + \beta^2}}$$

$$\sin \zeta \triangleq \frac{\beta}{\sqrt{\alpha^2 + \beta^2}} \quad , \tag{2.90}$$

where the angle ζ may be computed at once by virtue of Eqs. (2.88), we find that Eq. (2.89) can be written

$$\cos \zeta \cos \theta + \sin \zeta \sin \theta = \frac{\cos \psi - \gamma}{\sqrt{\alpha^2 + \beta^2}} \tag{2.91}$$

or

$$\cos(\zeta - \theta) = \frac{\cos \psi - \gamma}{\sqrt{\alpha^2 + \beta^2}} \quad . \tag{2.92}$$

Evidently, then

$$\theta = \zeta - \cos^{-1} \left[\frac{\cos \psi - \gamma}{\sqrt{\alpha^2 + \beta^2}} \right] \quad , \tag{2.93}$$

which is an equation with two zeros corresponding to the upper and lower branches of the visibility cone. (ψ is a rapidly changing function of time, whereas α, β, γ, and ζ are more slowly varying functions.)

From this point on one can compute the actual universal time of the critical photographic limits by the relation

$$\theta = \theta_c + \dot{\theta}(t - t_o) + \lambda_E \tag{2.94}$$

or

$$t = t_o + \frac{\zeta - \theta_o - \lambda_E}{\dot{\theta}}$$

where θ_o is an epoch sidereal time corresponding to t_o and $\dot{\theta}$ is the constant sidereal rate of change. The east longitude is as usual denoted by λ_E.

During the first attempts to photograph an unknown planet or moon, it may not be desired to photograph any particular area of the surface, but rather, any or all of the surface. The only constraint then is to operate the camera when the surface in the camera's view is properly illuminated. This problem is the more general case of the one just discussed and is solved as follows.

Replace $\underline{R}$ with $\underline{r}$ in Eq. (2.84) so that

$$\underline{r} \cdot \underline{R}_\odot = r R_\odot \cos(< \underline{R}, \underline{r}) \tag{2.96}$$

or in the orbit plane

LOCKHEED
CALIFORNIA COMPANY

$$(x_\omega \underline{P} + y_\omega \underline{Q}) \cdot \underline{R}_\odot = rR_\odot \cos \psi' \quad . \qquad (2.97)$$

For the ellipse,

$$x_\omega = a(\cos E - e)$$

$$y_\omega = \sqrt{1 - e^2} \sin E$$

$$r = a(1 - e \cos E)$$

where a, e, i, Ω, ω are the standard orbital elements and ψ' is the arbitrary angle spread between the Sun and satellites' radius vectors. Eq. (2.97) is actually

$$a(\cos E - e)\, \underline{P}\cdot\underline{R}_\odot + (a\sqrt{1-e^2} \sin E)\, \underline{Q}\cdot\underline{R}_\odot = a(1 - e \cos E)R_\odot \cos \psi' \qquad (2.98)$$

or

$$(\underline{P}\cdot\underline{R}_\odot + eR_\odot \cos \psi')\cos E + \sqrt{1-e^2}\, \underline{Q}\cdot\underline{R}_\odot \sin E = + e\, \underline{P}\cdot\underline{R}_\odot + aR_\odot \cos \psi' \qquad (2.99)$$

Therefore, if

$$\cos \alpha' \triangleq \frac{\underline{P}\cdot\underline{R}_\odot + eR_\odot \cos \psi'}{\sqrt{(\underline{P}\cdot\underline{R}_\odot + eR_\odot \cos \psi')^2 + (\sqrt{1-e^2}\, \underline{Q}\cdot\underline{R}_\odot)^2}}$$

$$\sin \alpha' \triangleq \frac{\sqrt{1 - e^2}\, \underline{Q}\cdot\underline{R}_\odot}{\sqrt{(\underline{P}\cdot\underline{R}_\odot + eR_\odot \cos \psi')^2 + (\sqrt{1-e^2}\, \underline{Q}\cdot\underline{R}_\odot)^2}}$$

$$\gamma' \triangleq \frac{e\,\underline{P}\cdot\underline{R}_\odot + aR_\odot \cos\psi'}{\sqrt{\left(\underline{P}\cdot\underline{R}_\odot + eR_\odot \cos\psi'\right)^2 + \left(\sqrt{1-e^2}\,\underline{Q}\cdot\underline{R}_\odot\right)^2}}$$

Eq. (2.99) reduces to

$$\cos\alpha' \cos E + \sin\alpha' \sin E = \gamma' \qquad (2.100)$$

or

$$\cos(\alpha' - E) = \gamma' \qquad (2.101)$$

so that

$$E_i = \alpha' - \cos^{-1}(\gamma') \qquad i = 1,2 \quad . \qquad (2.102)$$

This equation provides two zeros that are the limiting eccentric anomalies of the satellite at which the camera is to be turned on and off. The mapping from eccentric anomaly to time is now obtained from Kepler's equation, i.e.,

$$t_i = \frac{E_i - e \sin E_i}{k\sqrt{\mu}\; a^{-3/2}} + T \quad . \qquad (2.103)$$

It should be noted that the solution has assumed that the Sun's position did not change since the last time of perifocal passage of the satellite; i.e., $X_\odot$, $Y_\odot$, $Z_\odot$ were obtained from the Ephemeris tape at that point. The coordinates of the Sun do not vary much during the orbital period of a near Earth satellite. However, if higher accuracy is desired, an interpolation at the t_i obtained from

Eq. (2.103) will yield much more accurate values of the Sun's position, and the analysis can be repeated. More than one iteration will not be necessary.

SECTION III

CAMERA ORIENTATION

III-A: GENERAL REMARKS

Knowledge of the orientation of the optical axis of the camera in space is a prerequisite to the determination of scale and the location of objects photographed. Basically, there are two ways in which this problem may be attacked. One is through attitude sensing devices on board the satellite, and the other is through photogrammetric techniques utilizing ground control points.

It is not the purpose of this study to analyze in detail attitude control and sensing systems. However, a generalized discussion illucidating some problems and expectations is included here to broaden the reader's perspective.

III-3: ATTITUDE SENSING PROBLEMS FOR PHOTOGRAMMETRY FROM SPACE VEHICLES

For the purposes of photogrammetry from Earth satellites, lunar or planetary satellites or fly-by vehicles, some form of loose attitude control is necessary in order to point the photogrammetric sensors more or less in the right direction. However, the actual indexing of the location of a specific picture need not depend upon attitude control per se, but may involve only a knowledge of orientation at the time the picture was made. If one wishes to determine the location on the surface of a point in the picture, a knowledge of the space vehicle position is the first requisite, and a knowledge of its orientation is a second requisite; for the purposes of statistical combination, these can be considered independent variables.

If the control of the attitude of the entire vehicle - or at least the control of the photogrammetric sensors, if they are gimbaled relative to the vehicle - is sufficiently accurate in itself, then no further information is required concerning vehicle orientation at the time of taking the picture. For example, for an orientation error of 1° relative to the "local vertical" (which must be defined carefully in this context), a location error of about 17.45 kilometers occurs at a slant range of 1,000 kilometers. In order to obtain an error no greater than 0.5 kilometers from vehicle attitude errors at a slant

range of 1,000 kilometers, it is necessary to hold attitude within about 2 minutes of arc. On the other hand, even if the vehicle attitude is not controlled this accurately it can happen that orientation sensors provide a knowledge of orientation considerably better than that to which it is actually controlled. In this case, it is sufficient to record this sensor information with each picture or frame.

The following comments concern the attitude control and attitude sensing accuracies which might reasonably be expected in relatively close Earth satellites, lunar and planetary satellites, or fly-by vehicles. It is necessary to consider separately the cases of vehicles near the Earth or near a planet with an atmosphere and vehicles near the atmosphereless Moon. The difference between a satellite and fly-by situation is largely in the fact that the latter is a transient situation. But from the stand point of active closed loop attitude control, the transient is a relatively low frequency one and the control problems do not essentially differ in the two cases. Nor, for that matter, do the sensing problems differ except insofar as data might be collected at longer ranges from the planetary surface in the case of a fly-by.

It is desirable first to see how the three major methods of attitude stabilization might apply to this kind of operation. These are spin stabilization, passive or semi-passive stabilization, and active closed loop attitude control. Although spin stabilization has been used in the TIROS to obtain cloud cover pictures, the attitude

resolution is considerably poorer than would be appropriate for photogrammetry. Any developments that would permit the attainment of a considerably better resolution with a spinning vehicle are not known; hence, this class of attitude stabilization techniques is not appropriate to the present problem.

Passive and semi-passive stabilization, however, requires more consideration. The essential characteristics of such systems are two: a source of static stability from the natural environment of the vehicle must exist; a means must be provided for the dissipation of energy when the vehicle oscillates about the position of stable static equilibrium. Four potential sources of static equilibrium have been proposed and discussed in the passive stabilization literature and each has been made the subject of a complete concept for a passively stabilized vehicle. These sources are the gravity gradient effect, the Earth's magnetic field, the atmosphere, and solar radiation pressure. For photogrammetric purposes, the natural equilibrium should result in a stable orientation such that the photographic sensors can be pointed more or less "down" toward the nearby body. Only the gravity gradient and aerodynamic passive stabilization methods result in this kind of orientation for general orbits. The former would apply to any orbit or trajectory in the neighborhood of any gravitating source, the magnitude of the stabilizing torque being proportional to the square of the orbital frequency at the vehicles orbital radius and proportional to the difference in principle moments

of inertia of the vehicle (it being understood that the long axis, the one of minimum moment of inertia, is to be stabilized toward the central body). In a non-circular orbit, the gravity gradient torque is a function of time and does not really result in an orientation that is stable in the usual sense. Rather the situation is a dynamic one, one which has apparently not been given much attention. Methods based on the interaction of the vehicle with the ambient atmosphere are obviously inappropriate for lunar photogrammetry, but could work in the case of Mars. Here one must strike a fine balance between atmospheric effects that result in significant retardation and destruction of the orbit and atmospheric effects that are just sufficient to provide aerodynamic stability.

Certain facts regarding passive stabilization can be summarized. First, the existence of feasible physical means for providing the necessary passive damping has not yet been demonstrated. Second, no significant experience with passive stabilization in space has yet been acquired, although preliminary results for one particular type, that used on the TRAAC satellites are available. Third, there is virtually no extant analytical study of the passive stabilization method predicated upon a realistic dynamic model of the situation. Fourth, such analytical work as does exist indicates that attitude oscillations of some degrees can be expected - perhaps in the range of 5 to 20° about the vertical. It seems very unlikely at this time that a passive stabilization system could be designed and implemented,

capable of holding attitude within 3° of the vertical. The sum of these facts forces the conclusion that it would be very speculative to postulate passive attitude stabilization as a feasible basis for photogrammetry within the immediately foreseeable future. At the level of accuracy that seems to be realistic, one undoubtedly would need independent sensors to establish orientation for purposes of picture indexing. Once these sensors are added, one cuts deeply into the ostensible advantages of a passive stabilization system, namely its greater claimed reliability.

The remainder of the discussion will be concerned only with active closed loop attitude control and with the sensors that might be incorporated in such control systems.

For a near Earth satellite, an active closed loop attitude control system normally is based upon a horizon scanner to determine the vertical and a rate gyroscope to determine yaw. The control may be on-off if the actuators used with these sensors involve mass expulsion, or may be a proportional control if internal momentum storage devices are used or if proportional jets in the necessary thrust range became feasible. In the former case, the system operates in an attitude limit cycle whose amplitude is determined by practical considerations involving several characteristics: the width of the dead band introduced deliberately to conserve propellant, the minimum on-time of the thrusters used, and the threshold rates that can be detected by rate gyroscopes or by signal processing techniques

equivalent to them. The inherent accuracy of the sensor is also fundamental since there is no point in attempting to operate in a limit cycle much tighter than the inherent accuracy of the horizon scanner. Present scanners and those projected for the near future appear to have accuracies of the order of 1 to 2°. This includes the error effects of the inhomogeniety of the Earth's optical surface as well as instrument noise - the former appears to be the limiting factor in the spectral regions and with the instrument designs now used. The number does not represent an ultimate capability for this type of device, but should be typical for the purposes of the present discussion. This means that neither attitude control nor attitude sensing is likely to be better than 1 to 2° for near Earth satellites based on such a scheme. This is not likely to be adequate for photogrammetric purposes. In order to obtain significantly increased accuracy, one must go to attitude sensing by means of star trackers, a method which requires that a running knowledge of geographic position be present aboard the vehicle in order to know how to aim the lines of sight of the two or more trackers. This problem is more difficult than the attitude sensing problem for the Orbiting Astronomical Observatory vehicle, since there it is desired to point the vehicle axes in a prescribed direction in inertial space rather than toward the center of the Earth, and no changing angles between the vehicle axes and the star tracker lines of sight are involved. Changing angles are involved, however, for the photogrammetric problem.

Unfortunately, it does not appear at this time that there are any good alternatives for sensing in the region of intermediate accuracy between star trackers and horizon scanner. The inherent star tracker capability cannot be quoted without an error analysis of a specific system, since it is intimately involved with position determination errors as well as the basic errors of the trackers themselves, the latter being probably within a factor of 2 to 10 arc seconds, although this number probably can be reduced in practice if it is justified on the basis of the other system errors. The ground station can be expected to be an important, if intermittent, part of the sensing loop.

In the neighborhood of the Moon, one does not have the option of using an infrared horizon scanner of the type suitable for application near the Earth. It is possible that horizon scanners in the visible or blue regions will be developed, accompanied by a computed logic which permits an inference of the location of the center of the Moon from observations on a gibbous or cresent outline. However, such devices are not considered current state-of-the-art. If such a device were available and were to be used, the major errors might be in the variations of lunar topography, but any such errors are difficult to assess in the absence of a specific sensor design concept. In any case, it appears that the only method which might offer relatively good data on orientation is the star tracker method. At the Moon, sufficiently accurate tracking could be done from the Earth so that a

vehicle ephemeris would be available to use in conjunction with the star trackers. This would permit the application to evolve very much as for an Earth satellite and roughly comparable accuracies could be expected. It should be noted that such a technique would apply equally well to an orbit or to a hyperbolic trajectory in the Moon's neighborhood, provided the elements of this trajectory are established from the Earth with sufficient accuracy.

The case of planetary photogrammetry is somewhat more difficult. On one hand, the infrared horizon scanner might again become applicable if there is a suitable planetary atmosphere, but only fragmentary studies currently seem to be available on the problem of horizon scanning involving atmospheres other than the Earth's. Conjecturing that a method of this kind is feasible, it seems fairly safe to assume that rough location data would be forthcoming - locations to within an accuracy consistent with the 1 to 2° horizon scanner error that might be foreseen. But on the other hand, the higher accuracy sensing methods involving star tracking do not work as well because the establishment of an accurate planetary orbit from Earth-based observation is unlikely. This means that the star tracker attitude sensing would have to be supplemented by an onboard position determination method involving sightings on the planet, probably upon the Sun, and perhaps involving radio communication with the planetary surface.

It is difficult to go beyond these general remarks except in reference to a specific time period, a relatively specific mission

characterization, and more definitive photogrammetric requirements. First, attitude control tends to come in three levels of accuracy: sloppy (3 to 10°, possibly typical of a passively stabilized system); medium accuracy (1 to 2°, typical of average attitude control applications involving active closed loop control systems, and garden variety sensors); very accurate (probably better than . minute of arc when various sources of error are considered, requiring the use of star trackers). There seem to be no promising sensors in a range intermediate between horizon scanners and star trackers, although it is possible that horizon scanners could be made somewhat more accurate than the number quoted. (It is unlikely that the improvement would be an order of magnitude, though.) If the horizon scanning method were sufficiently accurate for the purposes of the photogrammetry, it could be used near the Earth and probably near other planets with atmospheres, but not for lunar photogrammetry with horizon scanners of current type. If horizon scanners are not sufficiently accurate for the purpose, one must perforce go to star trackers. These are potentially suitable for any of the neighborhoods mentioned, but if used near a distant planet they would have to be supplemented by an onboard position determination method.

III-C: CAMERA ORIENTATION FROM GROUND CONTROL

In the case of the moon and planets, ground control will range from poor to absent, and attitude sensing, discussed in the previous pages, will be the most expedient means of orientation. In the case of the Earth, ground control is fair to excellent (except for the polar regions) and can be used to great advantage in camera orientation.

Ideally, the position of ground nadir (subsatellite point) and satellite altitude will be known, because a precisely determined orbit and the exposure time are all that is required, as discussed in Section IV. Laboratory-processed Baker-Nunn observational data enable Earth satellite locations within one kilometer and this is sufficiently accurate for exploratory work considered in this study. The orientation of the low and high oblique photographs is considered separately.

PHOTOGRAMMETRIC DEFINITIONS AND SYMBOLS

Symbol	Term	Definition
	Apparent horizon	Outline of the Earth's horizon on an oblique photograph
θ	Depression angle	Vertical angle between the true horizon and the optical axes of the camera
d	Dip angle	Vertical angle between the true and apparent horizons
r_c	Earth's radius	
L	Exposure station	Position of the front nodal point of the lens at the time of exposure
f	Focal length	Distance from the front nodal point of the lens to the photographic negative
	Geodesic line	Shortest distance between two points on a mathematically defined surface (in this case a sphere)
G	Ground distance	
N	Ground nadir point	Point on the ground vertically beneath the exposure station
H	Height above datum	
	High oblique	Oblique photograph in which the Earth's horizon appears
	Low oblique	Oblique photograph in which the Earth's horizon does not appear

Symbol	Term	Definition
n	Nadir point	Point on the photograph vertically beneath the exposure station
	Nautical mile	(Historically) Distance on the Earth's equator subtending an angle of one minute at the Earth's center. (One nautical mile = 6080 feet.)
	Optical axis	Line perpendicular to the lens at the front nodal point
	Principal line	Line of intersection formed by the principal plane and the photograph
	Principal plane	Vertical plane containing the optical axis
O	Principal point	Point of intersection of the optical axis and the photograph
t	Tilt	Angle between the optical axis and the vertical
	Tilted photograph	Photograph taken with the optical axis of the camera inclined less than five degrees from the vertical. A distinction is commonly made between the tilted and the oblique photograph: tilt is an unintentional deviation from the vertical
	True horizon	Line of intersection of the horizontal plane through the exposure station and the photograph
S	Scale of photo	
I	Size of object in focal plane	

Symbol	Term	Definition
φ		Angle in the principal plane between the principal point and a horizontal line passing through the point of interest
e		Distance along the principal line in the photograph measured from the true horizon
β		Horizontal angle between two lines in an oblique photograph
ψ		Planetocentric angle subtended by an arc on the surface

High Oblique Photographs: Determination of Depression Angle and Azimuth of the Principal Line

The determination of the depression angle θ of the optical axis is a simple procedure in high oblique photographs. In fact, this is one of the advantages of a high oblique photograph. No ground control is necessary, nor is the location of ground nadir. Only the altitude and planetary radius are needed. The procedure can be found in most standard textbooks on photogrammetry; however, it is included here for the sake of completeness.

The angle between the apparent horizon and the true horizon is the dip angle d. (Refer to the previous two pages on Notation for definition of photogrammetric terms.) The dip angle is measured in the principal (i.e., vertical) plane containing the optical axis and the plumb line from the exposure station. As shown in Fig. 3.1, it is readily calculated from the flying height H and Earth's radius r_c:

$$\tan d = \frac{LK}{r_c} = \frac{\sqrt{(H + r_c)^2 - r_c^2}}{r_c}$$

$$= \frac{\sqrt{H^2 + 2r_c H}}{r_c} \qquad (3.1)$$

(Point K in the figure represents a point on the apparent horizon).

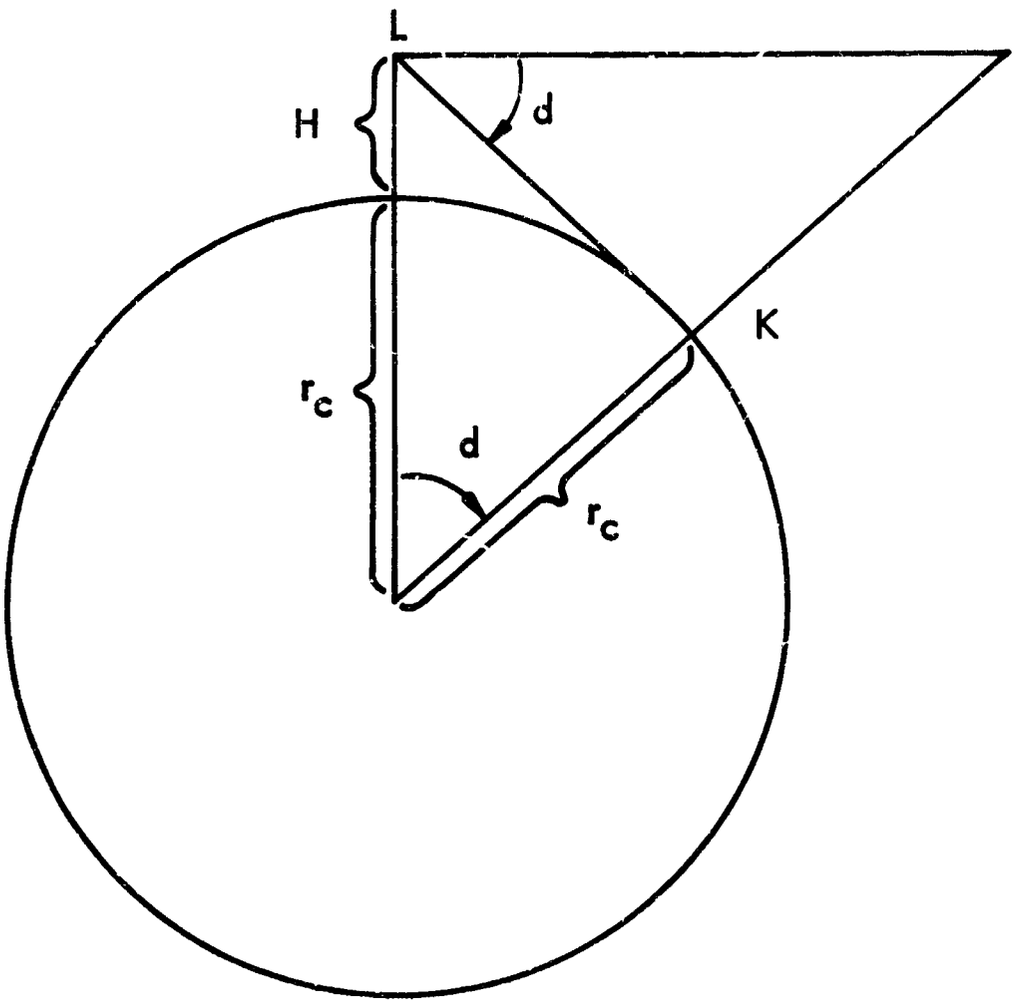

Figure 3.1: Relation of Dip Angle to Flying Height

The apparent depression angle α is measured in the principal plane between the apparent horizon and the optical axis, as shown in Fig. 3.2. If O is the principal point of the photograph, if follows from Fig. 3.2 that

$$\tan \alpha = \frac{OK'}{f} \tag{3.2}$$

The line OK' is measured along the principal point to the apparent horizon. (The interpreter can draw the principal line on the photo by constructing a line from the principal point perpendicular to the apparent horizon.) Experience shows that the Earth's horizon is not visible in hyperaltitude photographs. However, a fairly sharp line is formed at the top of the scattering layer of the atmosphere. It is expedient to measure OK' to this line and increase r_e in Eq. (3.1) by 12 km. The precise height of the scattering layer is not known, but in one of the Viking 12 photos it was estimated at about 12 km. for infrared.

The true depression angle between the optical axis and the horizontal is then readily determined:

$$\theta = \alpha + d \tag{3.3}$$

Now the true horizon is located by

$$OM = f \tan \theta \quad , \tag{3.4}$$

and the nadir point of the photograph by

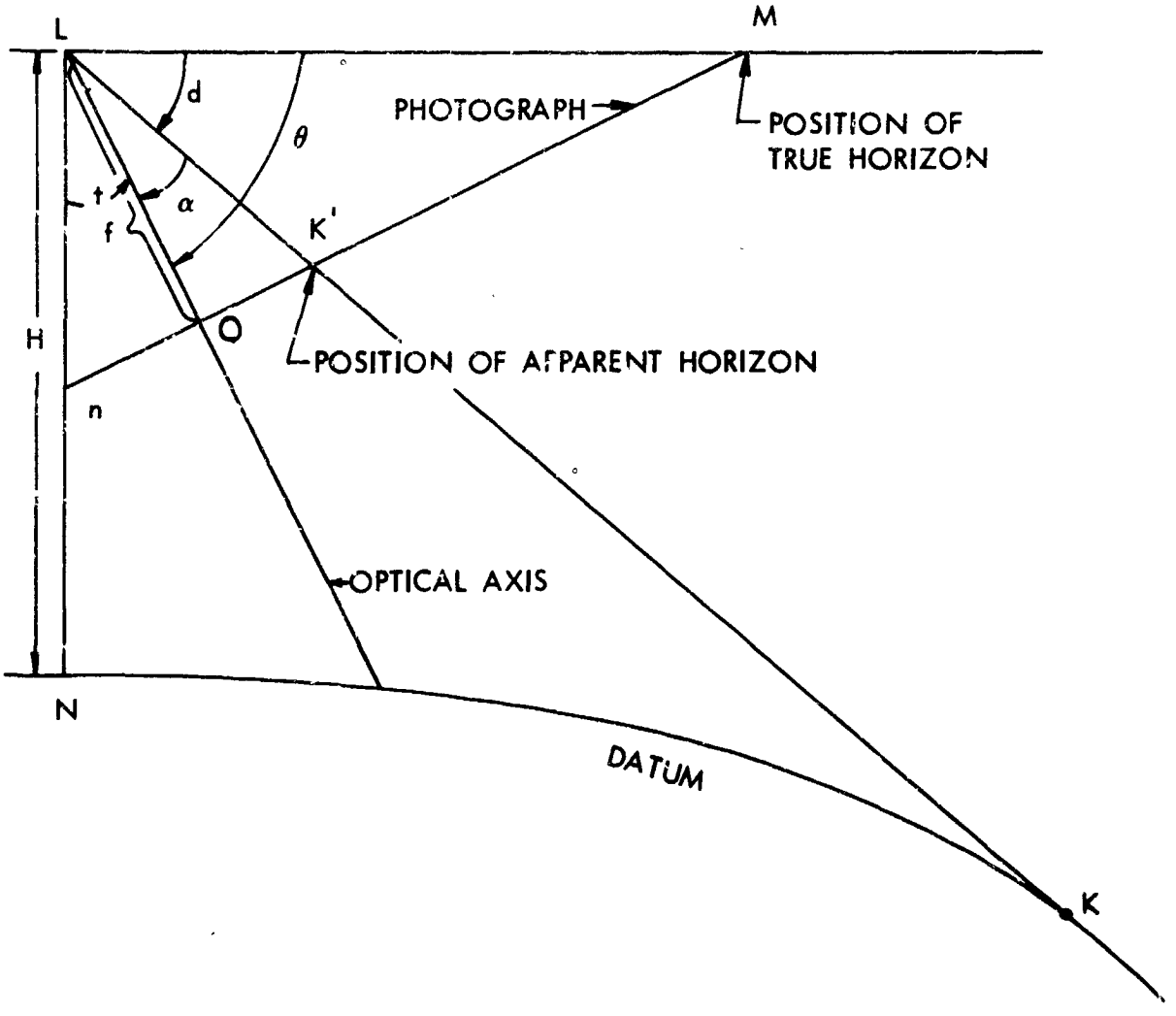

Figure 3.2: Elements of the High Oblique Photograph

$$On = f \tan t \quad , \tag{3.5}$$

where t is the tilt found by

$$t = 90^{\circ} - \theta \quad . \tag{3.6}$$

To complete the orientation of the camera in space, the azimuth of the principal line must be determined. This is easily accomplished if a recognizable ground point lies along the principal line of the photograph. A line from ground nadir through the recognized point can then be plotted on a map to determine its direction. However, any control point in the photograph is sufficient, in addition to the coordinates of ground nadir, for determining the azimuth. The line connecting ground nadir with the control point is considered the control line and its direction is determined. The direction of a line can be determined directly from a Mercator map, or more generally, by Napier's analogies. The problem, which is common in navigation, is shown in Fig. 3.3. The desired angle in Fig. 3.3 is A, which is the direction of the control line measured from north.

By Napier's analogies,

$$\begin{aligned} \tan \frac{B + A}{2} &= \frac{\cos \frac{b - a}{2} \cdot \cot \frac{N}{2}}{\cos \frac{b + a}{2}} \\ \tan \frac{B - A}{2} &= \frac{\sin \frac{b - a}{2} \cdot \cot \frac{N}{2}}{\sin \frac{b + a}{2}} \end{aligned} \tag{3.7}$$

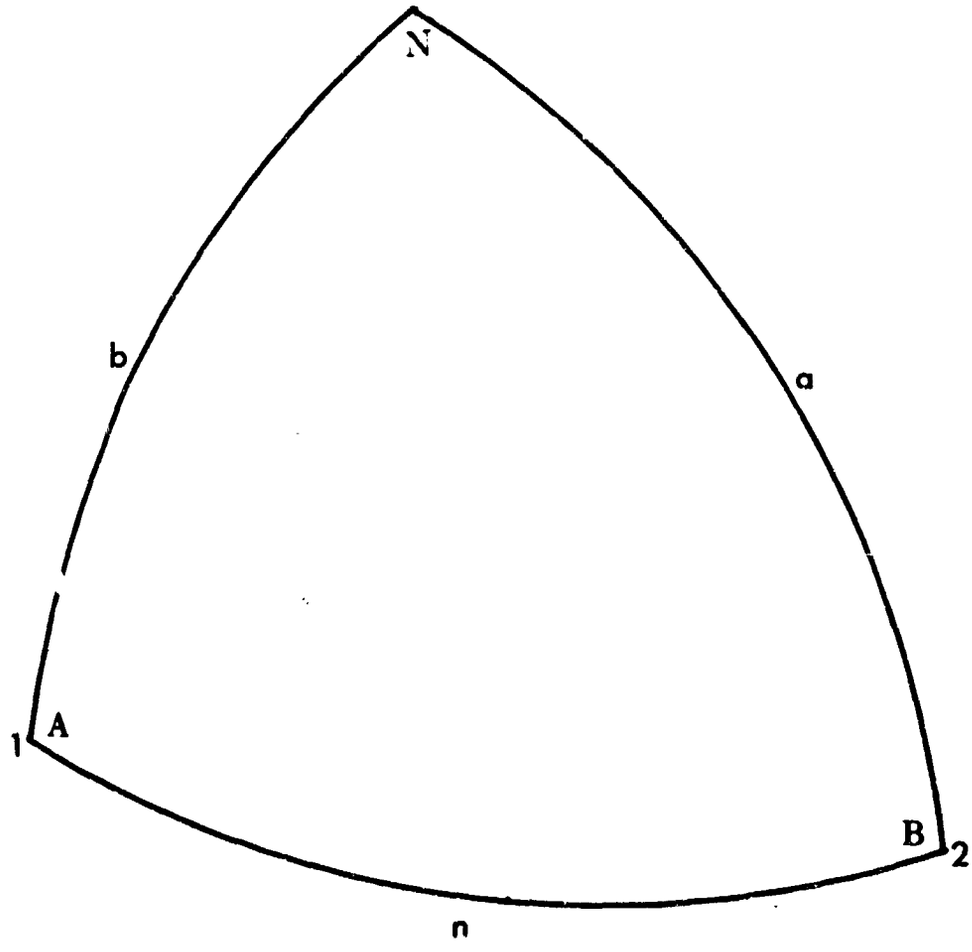

Figure 3.3: Spherical Triangle Formed by Principal Point (Point 1), Control Point (Point 2), and the Earth's North Pole

where

$$a = |90 - \varphi_2|$$

$$b = |90 - \varphi_1|$$

$$N = |\lambda_2 - \lambda_1| \quad .$$

Equations (3.7) are solved simultaneously for B and A.

The next step in finding the azimuth of the principal line when it cannot be identified by inspection on the map is to determine the horizontal angle β between the principal line and the control line, with the apex at ground nadir.

$$\tan \beta = \frac{x}{f \sec \theta + e \sin \theta} \tag{3.8}$$

where x is the distance to the control point measured in the x direction of the photograph, f is the focal length, and e is the distance along the principal line in the photograph from the true horizon to the control point (see Fig. 3.4).

The distance e is always negative in Eq. (3.8), because it is measured below the true horizon. See Moffitt, 1959, p. 342 for derivation of Eq. (3.8). The quantity e, as seen in Fig. 3.4 is equal to

$$- f \tan \theta \pm y \quad ,$$

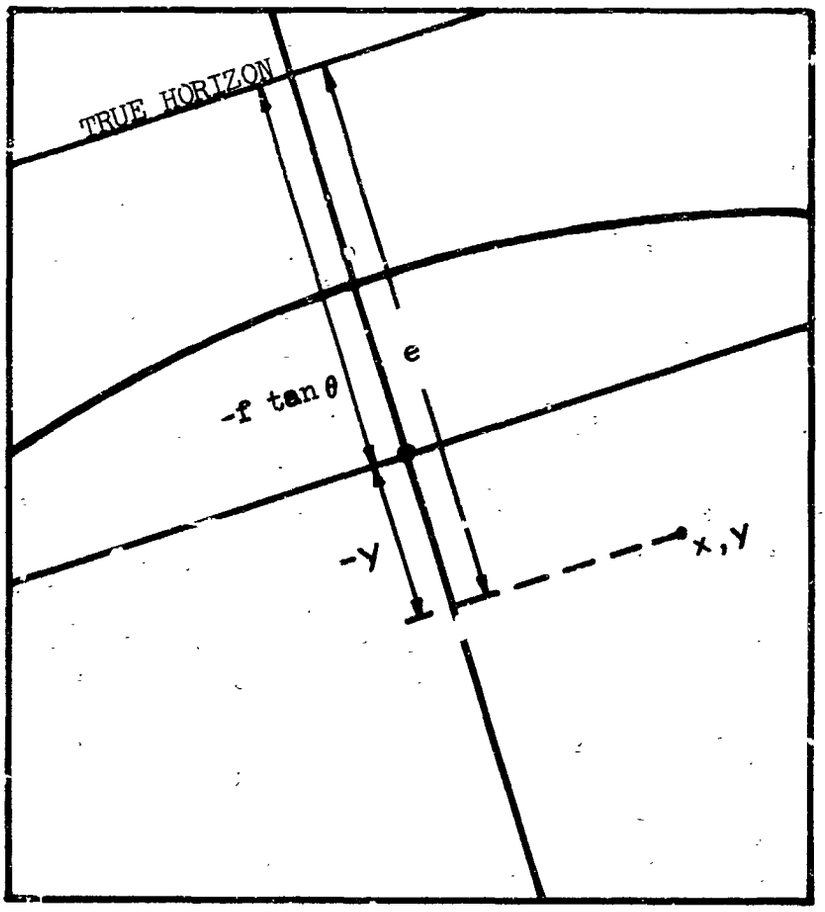

Figure 3.4: Determination of e.

where y is added if the control point lies below the principal point and subtracted if it lies above the principal point.

The angle β is then added or subtracted from the azimuth of the control line to find the azimuth of the principal line. For example, in Fig. 3.3 the azimuth of the control line is A, the azimuth being measured clockwise from north. The angle β would be subtracted if the control point lies south of the principal line and added if it lies north of the principal line.

Low Oblique: Tilt and Azimuth Determination

Orienting low oblique photographs is much more difficult than high obliques. However, if good maps of the photographed area are available it is commonly possible to locate the principal point of the photograph on a map, in which case the orientation is greatly simplified. Let us first consider this case in which the altitude of the satellite is known and both the ground nadir and the principal point of the photo can be plotted on a map. The geodetic distance n between ground nadir N and the principal point O is determined from

$$\tan \frac{n}{2} = \frac{\sin \frac{B + A}{2} \cdot \tan \frac{b - a}{2}}{\sin \frac{B - A}{2}} \qquad (3.9)$$

where A and B are found from Eq. 3.7.

Referring to Fig. 3.5, in which t is the tilt, H is the altitude of the satellite, r_c is the Earth's radius, and ψ is the central angle subtended by the geodetic arc n ($\psi_{radians} = \frac{n}{r_c}$),

$$\tan t = \frac{r_c \sin \psi}{H + r_c(1 - \cos \psi)} \quad . \tag{3.10}$$

For less precise work, it may be appropriate to measure the azimuth of the principal line and the distance n directly from the map, in which case the accuracy will depend on the quality and type of projection of the map. Furthermore, for small angles of tilt, the curvature of the Earth can be neglected and the tilt found as

$$t = \tan^{-1}\left[\frac{n}{H}\right] \tag{3.11}$$

The graph, Fig. 3.6, compares the precise determination, Eq. (3.10). with the approximation, Eq. (3.11), using the Earth as an example. The graph shows results using altitudes of 500 km and 1000 km.

Next the principal line is to be located on the photo. From careful comparison of the principal line plotted on the map with the photo, it may be possible to identify a point on the photo which lies along the principal line shown on the map. If this is the case, the principal line on the photo is constructed by extending a line through this point and the principal point.

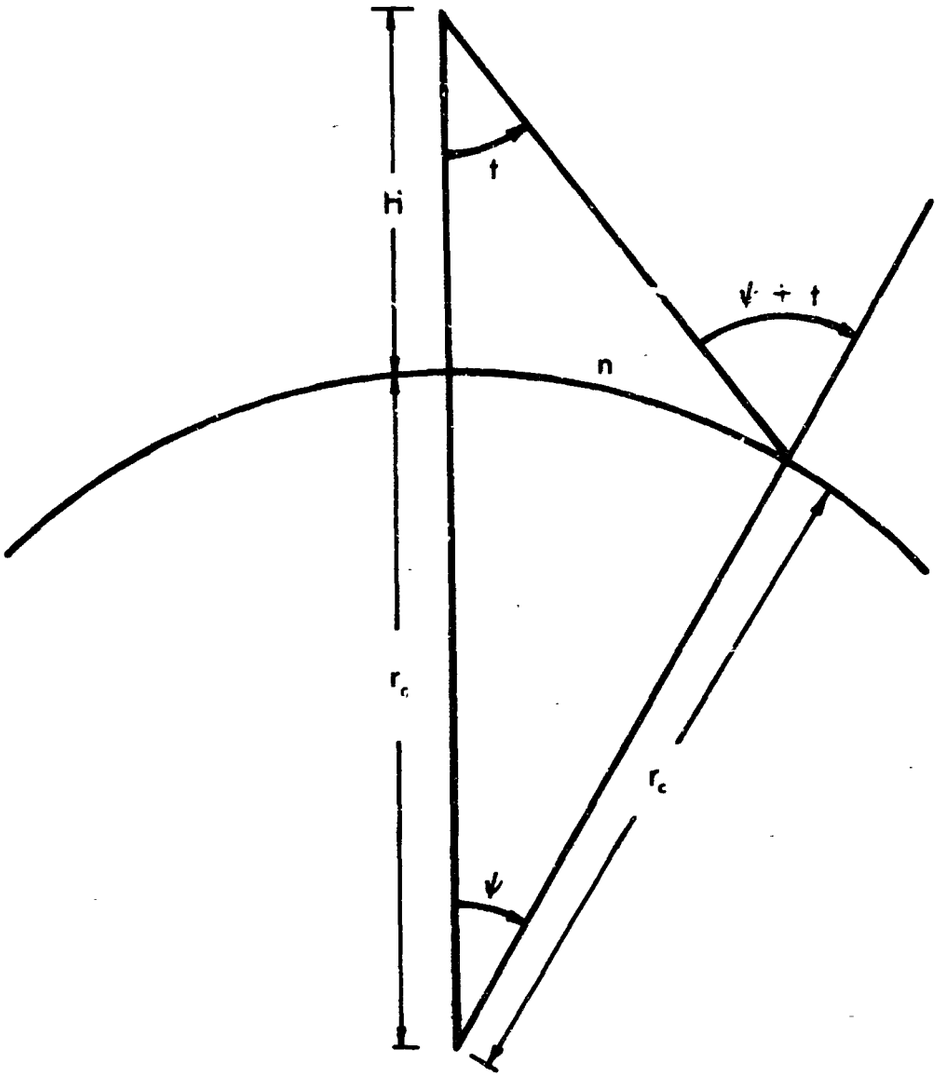

Figure 3.5: Determination of Tilt

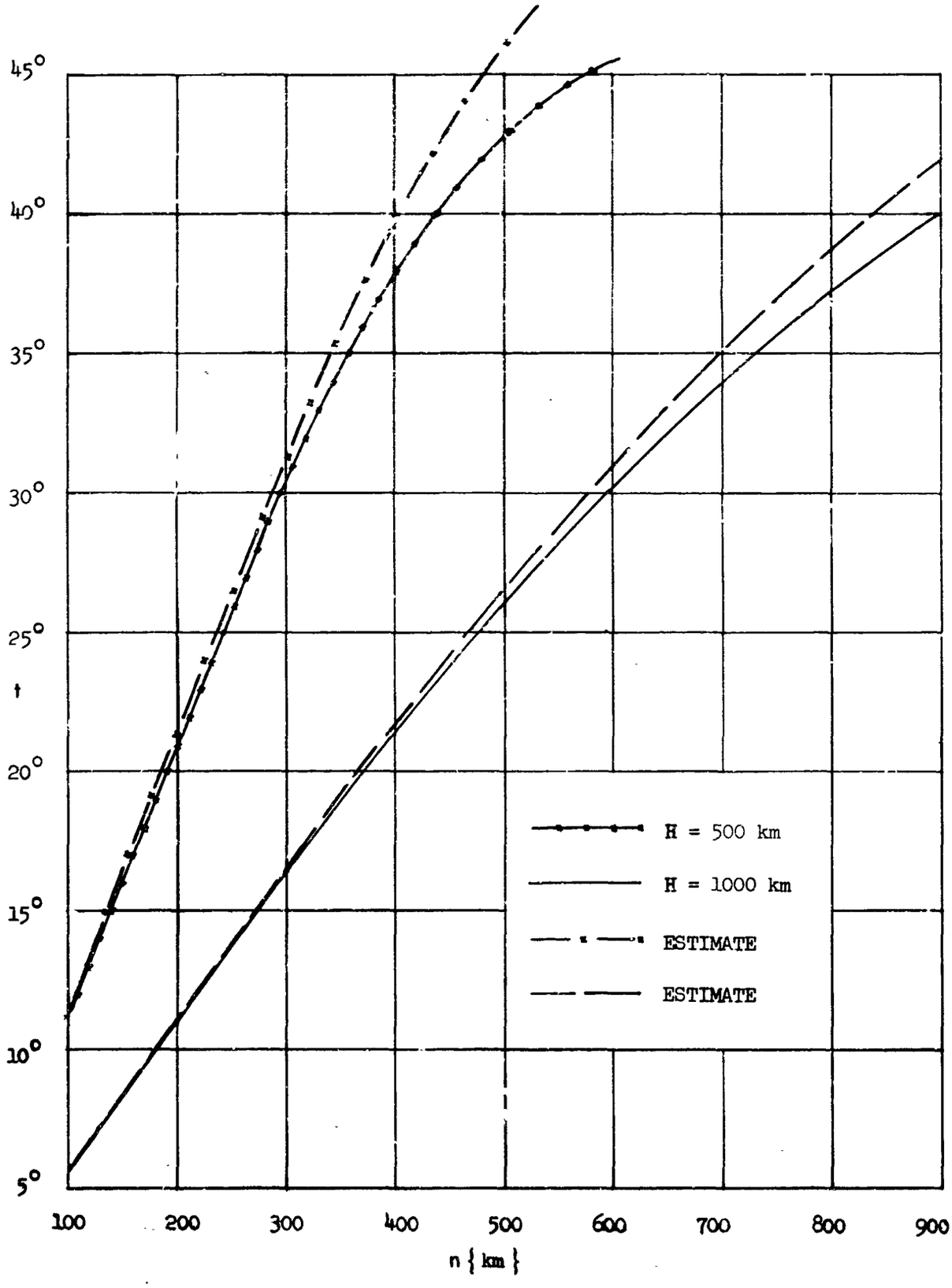

Figure 3.6: Approximate vs. True Tilt

If such a point cannot be identified, the principal line can be constructued if any other point in the photo can be recognized and located on the map. A line from the principal point to the control point is considered the control line, and the angle between this line and the principal line is the desired angle. This angle cannot be measured directly from the map; rather, the desired angle is the perspective projection of the map angle on a plane parallel to the photo. The problem is illustrated in Fig. 3.7. In this figure, the control point lies above the principal point. Consider first the case in which the curvature of the surface is neglected. A set of coordinate axes is constructed on the map, in which the Y axis coincides with the ground trace of the principal plane, and the X axis is perpendicular to Y at the principal point on the map. From the geometry of the figure, the projections of the X and Y distances of the control point on a plane parallel to the photo are

$$Y' = H \operatorname{sect} \tan \varphi \tag{3.12}$$

$$X' = \frac{X \cos(t + \varphi)}{\operatorname{cost} \cos \omega} \tag{3.13}$$

where

$$\varphi = \tan^{-1}\left[\frac{H \tan t + Y}{H}\right] - t \tag{3.14}$$

The smaller angle between the control line and the principal line in the plane of the photo, call it Δ, is then

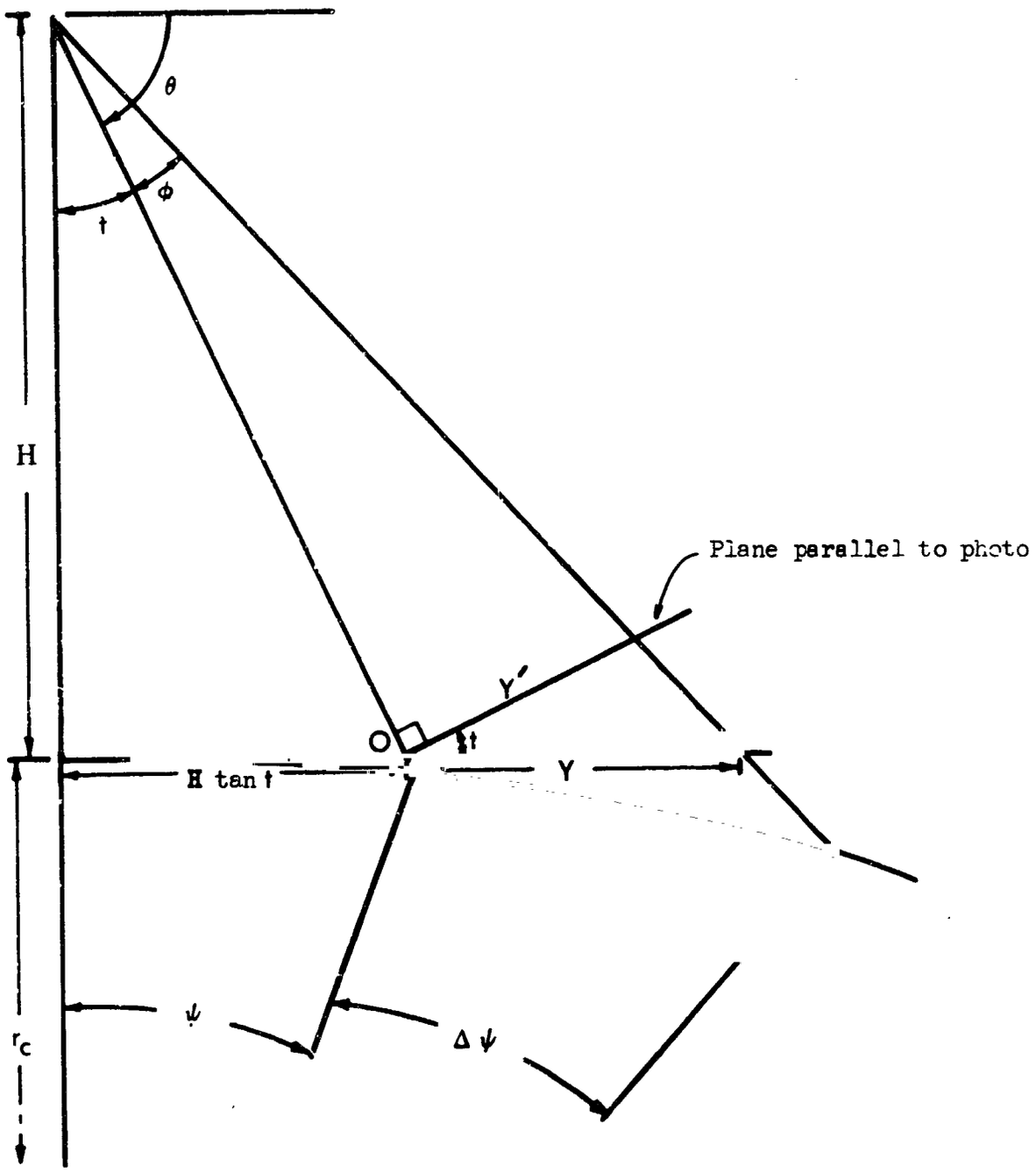

Figure 3.7: Projection of Y into the Plane of the Photo.
(Section in Principal Plane)

$$\Delta = \tan^{-1}\left[\frac{X'}{Y'}\right] \tag{3.15}$$

If the control point lies below the principal point, Eq. (3.12) is the same, but Eqs. (3.13) and (3.14) become

$$X' = \frac{X \cos(t - \varphi)}{\text{cost} \cos \varphi} \tag{3.16}$$

and

$$\varphi = \tan^{-1}\left[\frac{H \tan t - Y}{H}\right] - t \tag{3.17}$$

In the case of the Earth, the curvature should be considered in order to maintain an accuracy of one to two percent for tilts greater than about 30 degrees. Referring again to Fig. 3.7, but considering now the arc distance from the control point (projected into the principal plane) to the point where the optical axis intersects the surface, the angle φ, which is to be used in Eq. (3.12) is found from

$$\varphi = \tan^{-1}\left[\frac{r_c \sin(\psi + \Delta\psi)}{H + r_c\left[1 - \cos(\psi + \Delta\psi)\right]}\right] - t \tag{3.18}$$

where

$$\psi = \sin^{-1}\left[\frac{r_c + H}{r_c} \sin t\right] - t \quad , \tag{3.19}$$

and $\Delta\psi$ (in radians) is found by measuring the distance on the map between the ground location of the principal point and the projection of the control point into the ground trace of the principal plane, and

dividing this distance by the radius of the Earth. The effect of curvature in the X direction is negligible; nevertheless, it must be corrected to a perspective projection onto the plane parallel to the photo. If X is the distance measured from the map, and X' the perspective projection onto the plane parallel to the photo,

$$X' = \frac{XH \sin(t + \varphi)}{r_c \sin(\psi + \Delta\psi)\cos t \cos \varphi} \tag{3.20}$$

If the control point lies below the principal point, the effects of curvature will be much less than in the previous case; nevertheless, the projected distances are calculated similarly, except that Eq. (3.18) becomes

$$\varphi = t - \tan^{-1}\left[\frac{r_c \sin(\psi - \Delta\psi)}{H + r_c\left[1 - \cos(\psi - \Delta\psi)\right]}\right] \tag{3.21}$$

and Eq. (3.20) becomes

$$X' = \frac{XH \sin(t - \varphi)}{r_c \sin(\psi - \Delta\psi)\cos t \cos \varphi} \tag{3.22}$$

When the principal point is not easily located on a map, the problem of orientation becomes more difficult. If the altitude and ground nadir of the exposure station are known, orientation can be accomplished from two ground control points. A method for this situation is developed in the Westinghouse report to N.A.S.A. (NAS-5-2755).

If the altitude and ground nadir at the time of exposure are not known (as is the case with the Mercury-Atlas photos), the orientation of the photo can be determined from three ground control points in the photo.

The most useful features for ground control points in hyper-altitude photography have been found to be the irregular edges of bodies of water (lakes, reservoirs and coastlines), stream intersections, and road and railroad intersections or bends. The control points should be chosen to form a strong, i.e., nearly equilateral, base triangle. The resulting space pyramid formed by the ground control points and the camera station is then as strong as possible, providing that the camera station does not fall on the "critical cylinder", i.e., the vertical cylinder formed by the three control points. (An analogous situation can be demonstrated in surveying. The location of a resected station cannot be resolved if it falls on the circumference of the circle passing through the three control points.)

The commonly used orientation methods do not consider the curvature of the surface. For expectable altitudes of photographing satellites (below 1000 km.), significant error will not be introduced provided the points form angles of less than 30 to 40 degrees to the local vertical. After some experience with oblique photographs, the direction to the nearest horizon and the angle to the vertical can be estimated roughly by examining the amount of foreshortening at various

points in the photo. The control points should then, if possible, be selected in the lower (larger-scale) portion of the photograph.

The "scale-point method" of R.O. Anderson, described in Moffitt, 1959, pp. 213-221 and in the Manual of Photogrammetry, pp. 372-375, is mainly graphical, but is accompanied by simple mathematics. The method is useful if an electronic computer is not available; even so, it is time-consuming (particularly if the tilt is more than a few degrees), and because of the graphical operations, high precision is not to be expected.

More suitable are the analytical methods, such as the space resection method developed by the late Professor Earl Church of Syracuse University. The resection procedure implies determination of the elements of exterior orientation that allow the three reconstructed rays from the camera station to be adjusted in perspective position with the respective control points. The method is described in the Manual of Photogrammetry, 1952, pp. 275-280.

Another method, that of Lehman, 1963, was adapted and utilized successfuly for several rocket photos taken over White Sands, New Mexico. A computer program, as well as a flow diagram of the Lehman method are found in the Appendix of this report. The measurements on the photo should be made as precisely as possible, preferably on a precision comparator, and the effective focal length (i.e., after enlargement) must be known very accurately in order for the program to work effectively.

A third method of orientation for low obliques can be suggested and although it has not yet been attempted for hyperaltitude photography, it may prove to offer a rapid and satisfactory solution to the problem of reconstructing the original tilt and swing. The method is optical-mechanical reconstruction of tilt and swing in a precision rectifying projector. This is accomplished in the rectifying instrument by means of systematic trial and error adjustment of the projection easel so that the images of the control points on the photograph are brought into coincidence with the ground control points, which are plotted on the base sheet and positioned on the easel. The base control points are plotted from map or survey data and should be chosen at approximately the same elevation, unless the plotted positions are corrected for relief displacement, (see Moffitt, 1959, pp. 242-245).

SECTION IV

LOCATION OF OBJECTS IMAGED

IV-A: THE CONCEPT OF SCALE

It will be seen in the next section that objects can be located and distances between objects determined in a photograph without knowledge of scale. Nevertheless, scale is a fundamental property which aids us in describing a photograph in terms that are familiar and meaningful. Furthermore, estimates of size and distance are possible without tedious calculations, if the scale is known.

As generally used, scale is defined as the ratio of image distance to ground distance. That is, it is the ratio of the distance between two points as measured on a photograph to the actual distance between the same points on the ground. The reciprocal of this ratio is the scale number, which is more useful than scale, because image distance multiplied by scale number yields true ground distance:

$$G = S_i \times (\text{image distance}), \qquad (4.1)$$

where G is the ground distance and S_i is the scale number of the photograph. Throughout this study, scale number is used instead of scale.

In a vertical photograph, the scale number at the principal point is

$$S_v = \frac{H}{f}, \qquad (4.2)$$

where H is the altitude of the exposure station and f is the focal length of the camera (not to be confused with f, standing for Earth flattening). Outward from the principal point, the scale changes by a small amount owing to the curvature of the Earth and relief displacement.

In the nonvertical photograph the scale is different at each point, with the exception of all points along any single line perpendicular to the principal line. The scale number (S_i) of a point on an oblique photograph can, therefore, be defined as the change in ground distance relative to a change in image distance:

$$S_i = \frac{dG}{dI} \quad . \tag{4.3}$$

Only for measurements involving very small distances can the scale be considered constant, the limiting distances being commensurate with the accuracy desired.

It is convenient to refer the photograph to an appropriate coordinate system in x and y, in which the y axis coincides with the principal line. (The position of the x axis is arbitrary, but generally passes through the principal point or coincides with the true horizon. It is then expedient to examine how the scale number changes in the x direction (S_x) and in the y direction (S_y):

$$S_x = \frac{dX}{dx} \tag{4.4}$$

and

$$S_y = \frac{dY}{dy} \tag{4.5}$$

where X and Y are the ground distances and x and y are the corresponding image distances. As mentioned previously, the scale is invariant in the direction perpendicular to the principal line - a characteristic of perspective projection. Consequently, the scale in the x direction is constant, and the ground distance

$$X = S_x(x_2 - x_1) \quad , \tag{4.6}$$

where x_1 and x_2 are the image coordinates of the two points between which the distance is to be determined.

However, the scale changes continually in the y direction; therefore, a distance on the ground parallel to the principal plane is the definite integral of the scale number as a function of y.

$$y = \int_{y_1}^{y_2} S_y \, dy \quad . \tag{4.7}$$

It remains to derive expressions for S_x and S_y in terms of known or readily determined quantities. Such derivations have been carried out previously (by Katz in 1950, Lane in 1950, and Moffitt in 1959) and will not be repeated here. The geometry of the situation is seen in Figure 4.1.

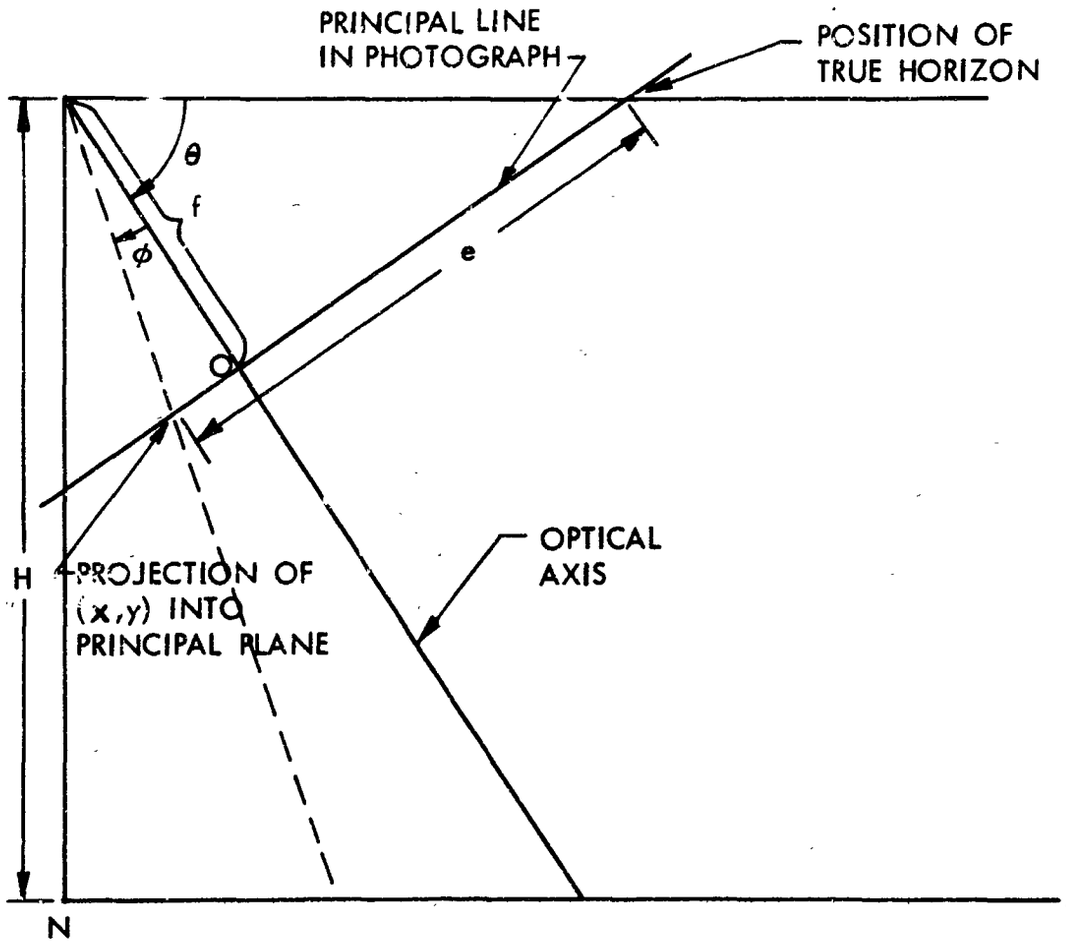

Figure 4.1: Elements of Scale

$$S_x = \frac{H \cos \varphi}{f \sin(\theta + \varphi)} \tag{4.8}$$

$$S_y = \frac{H}{f} \left[\frac{\cos \varphi}{\sin(\theta + \varphi)} \right]^2 \tag{4.9}$$

where S_x and S_y are the instantaneous scale numbers at a point; H equals focal length, θ equals depression angle; and φ equals the angle in the principal plane between the principal point, O, and a horizontal line passing through the point of interest.

The angle φ is considered positive when measured downward and negative when measured upward from the principal point.

The scale numbers can also be represented in terms of the image distance e from the true horizon rather than the angle φ (see Figure 4.1); from this, relatively simple expressions are obtained.

$$S_x = \frac{H}{e \cos \theta} \tag{4.10}$$

$$S_y = \frac{Hf}{e^2 \cos^2 \theta} \tag{4.11}$$

where H, f, and e are measured in the same units.

The concept of scale was found to be especially useful in this study in analyzing interpretability of photographs. For example, what scales are suitable for interpreting drainage, surficial deposits, rock strata, etc.?

IV-B: COORDINATES OF OBJECTS IMAGED

Once the orientation of the photograph in space is known, the location of any point in the photograph can be determined relative to ground nadir. The method developed here utilizes the theorems of solid analytic geometry and is readily adapted to the use of an accurate coordinate-measuring device, e.g., a comparator, and the hand calculator.

Referring to Fig. 4.2, consider two sets of three-dimensional coordinate axes, each having its origin at the front nodal point of the camera. One set of axes defines ground points, with the Z-axis parallel to the plumb line. The second coordinate system defines points on the photograph with the z-axis coincident with the optical axis. Ground points are designated $P_1(X_1, Y_1, Z_1)$, $P_2(X_2, Y_2, Z_2)$, etc. Image points are designated $p_1(x_1, y_1, z_1)$, etc. A ray from an object on the surface at P_1 to the exposure station pierces the photograph at p_1. The basic problem is to find the coordinates of P_1, knowing the coordinates of p_1.

In order to simplify the equations, the y-axis of the photograph as well as the Y-axis of the ground system are made to lie in the principal plane.

After measuring the x and y coordinates of the point in the photograph, the coordinates of this point are found in the ground

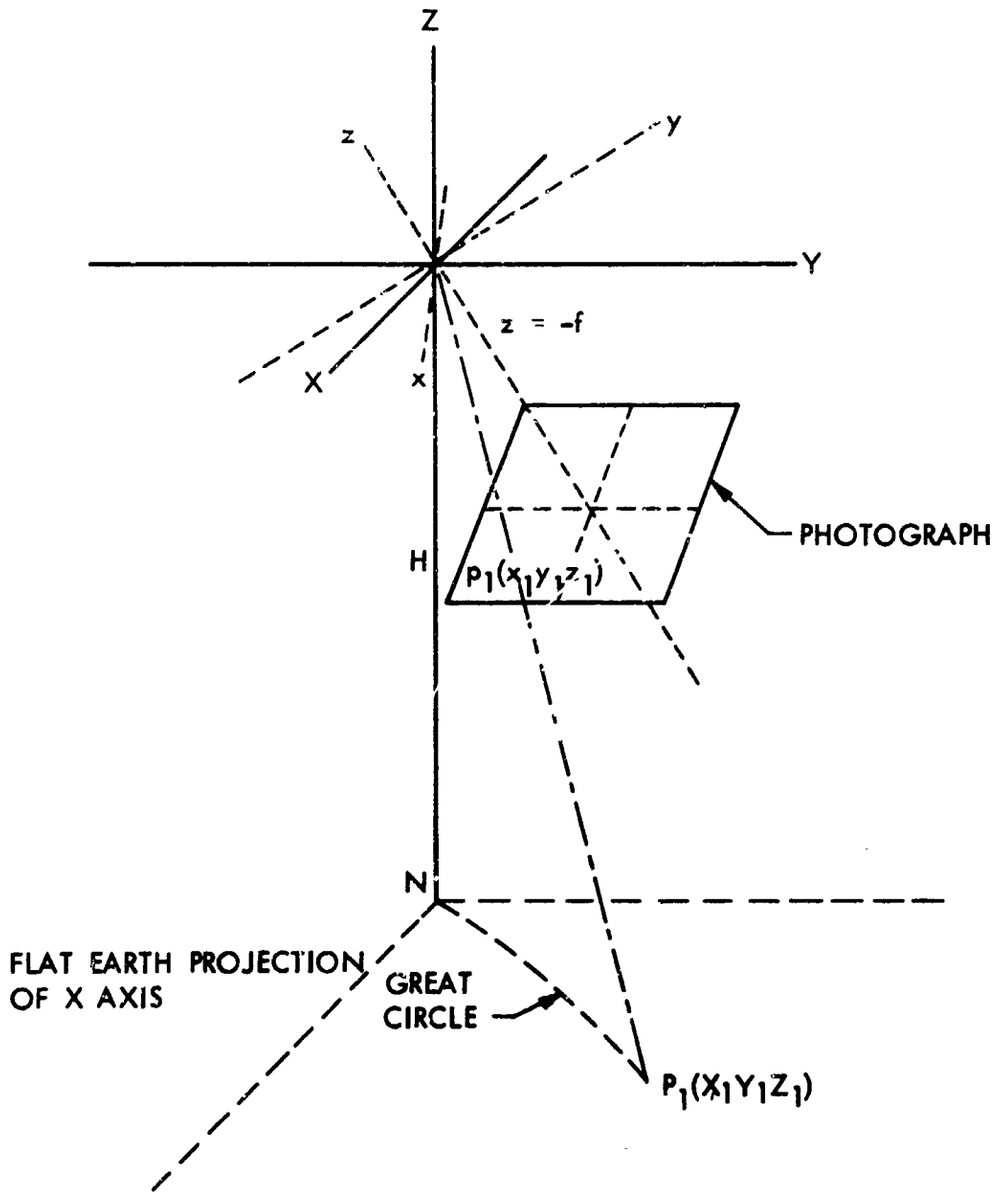

Figure 4.2: Relation of Photographic and Ground Coordinate Systems.

coordinate system, call them x', y', z'. This is accomplished by a simple rotation of the photographic coordinate frame about the x-axis through the angle of tilt, t.

$$\left.\begin{aligned} x' &= x \\ y' &= y\cos t + z\sin t \\ z' &= -y\sin t + z\cos t \quad . \end{aligned}\right\} \qquad (4.12)$$

Next, the parametric equations of the ray joining P_1 and the exposure station are determined. Calling k a parameter,

$$\left.\begin{aligned} x &= x'k \\ y &= y'k \\ z &= z'k \end{aligned}\right\} \qquad (4.13)$$

At the point $P_1(X_1, Y_1, Z_1)$, where the ray intersects the terrestrial (or planetary) sphere,* the coordinates of P_1 must satisfy the equation

$$r_c^2 = x^2 + y^2 + \left[z - (H + r_c)\right]^2 \quad , \qquad (4.14)$$

which is the equation of the terrestrial sphere relative to the XYZ coordinate axes in Figure 4.3.

The parametric forms of x, y and z (Eq. 4.13) are substituted in Eq. (4.14) which is solved for k. Next the coordinates of P_1

---

* Consideration of flattening will ordinarily not be warrented; however, for greater precision, the equation of the spheroid can be used instead of Eq. (4.14).

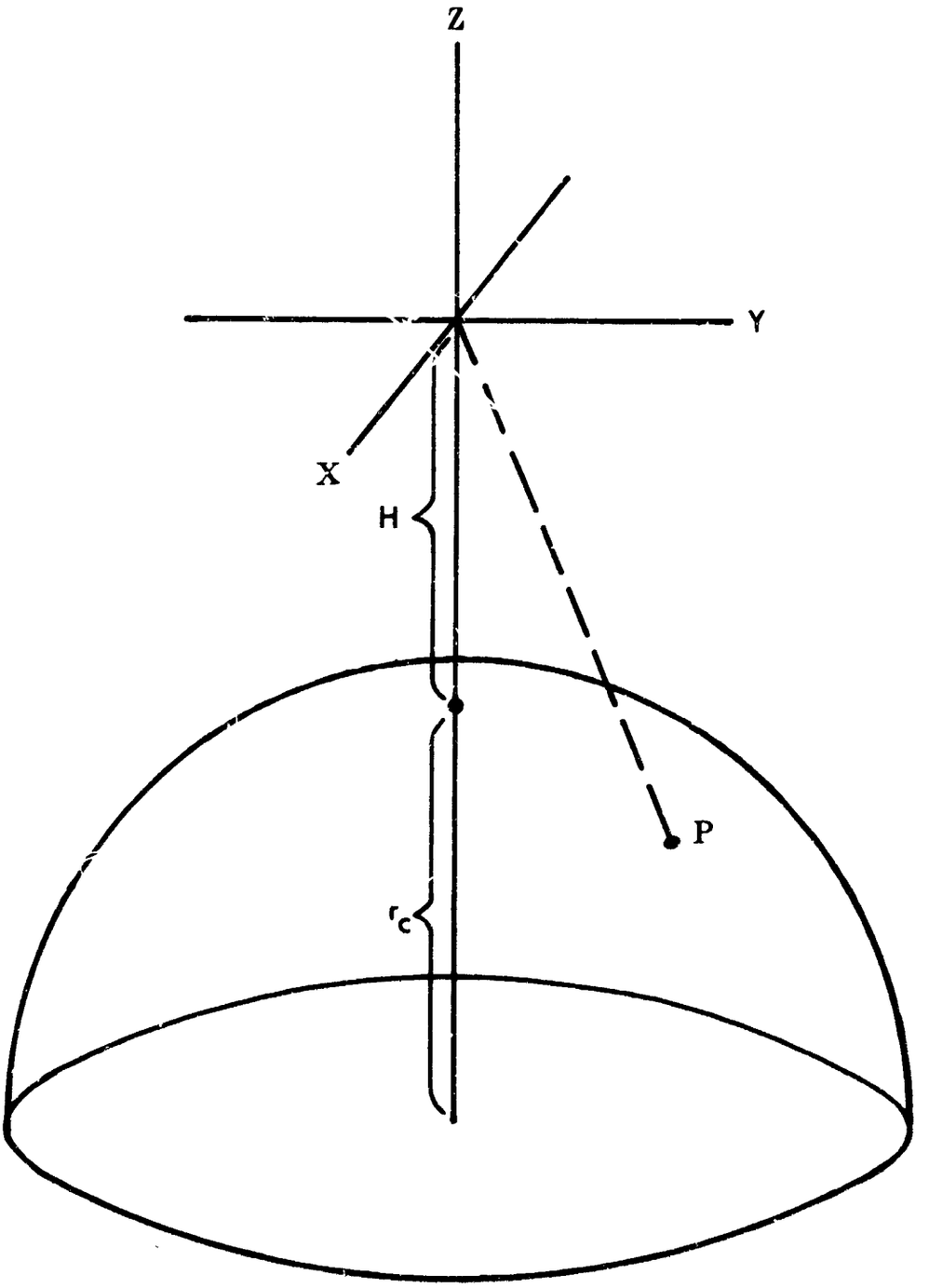

Figure 4.3: Ray From P to Exposure Station

are found from

$$\left.\begin{aligned} X &= x' k \\ Y &= y' k \\ Z &= z' k \quad . \end{aligned}\right\} \qquad (4.15)$$

In many cases it will be desirable to determine the coordinates of P_1 in the geodetic coordinate system of the planet, i.e., longitude λ and latitude φ. The XYZ coordinate system is rotated about the Z axis so that the X and Y axes coincide with the North-South and East-West directions. The new coordinates are designated X' and Y'.

$$X' = X \cos \epsilon + y \sin \epsilon \qquad (4.16)$$

$$Y' = -X \sin \epsilon + y \cos \epsilon \qquad (4.17)$$

where ϵ is the angle between North and the X axis. Then,

$$\Delta\varphi = \sin^{-1}\left[\frac{X'}{r_c}\right] \qquad (4.18)$$

$$\Delta\lambda = \sin^{-1}\left[\frac{Y'}{r_c} \sec L\right] \qquad (4.19)$$

where L is the latitude of ground nadir.

Finally

$$\lambda = \lambda_n + \Delta\lambda \qquad (4.20)$$

$$\varphi = \varphi_n + \Delta\varphi \qquad (4.21)$$

where φ_n and λ_n are the coordinates of ground nadir. $\Delta\lambda$ is positive westward in the western hemisphere, and $\Delta\varphi$ is positive northward in the northern hemisphere.

In Fig. 4.5, which is the plane containing the object and the ground nadir, D represents the displacement of an object P owing to its elevation above the datum. Clearly, the relief displacement increases with increasing elevation of the object and increasing distance from the ground nadir. Taking the Earth as a sphere,

$$D = \Delta\psi$$

where D is in nautical miles and $\Delta\psi$ is in minutes of arc.

In triangle LCP, from the law of sines,

$$\frac{\sin\delta}{r_c + h} = \frac{\sin(\psi + \delta)}{r_c + H}$$

$$\psi = \sin^{-1}\left[\frac{(r_c + H)\sin\delta}{r_c + h}\right] - \delta \quad . \qquad (4.24)$$

In triangle LP'C

$$\frac{\sin\delta}{r_c} = \frac{\sin(\delta + \psi + \Delta\psi)}{r_c + H}$$

$$\Delta\psi = \sin^{-1}\left[\frac{(r_c + H)\sin\delta}{r_c}\right] - \psi - \delta \qquad (4.25)$$

combining Eq. (4.24) and Eq. (4.25), we find that

$$\Delta\psi = \sin^{-1}\left[\frac{(r_c + H)\sin\delta}{r_c}\right] - \sin^{-1}\left[\frac{(r_c + H)\sin\delta}{r_c + h}\right] \qquad (4.26)$$

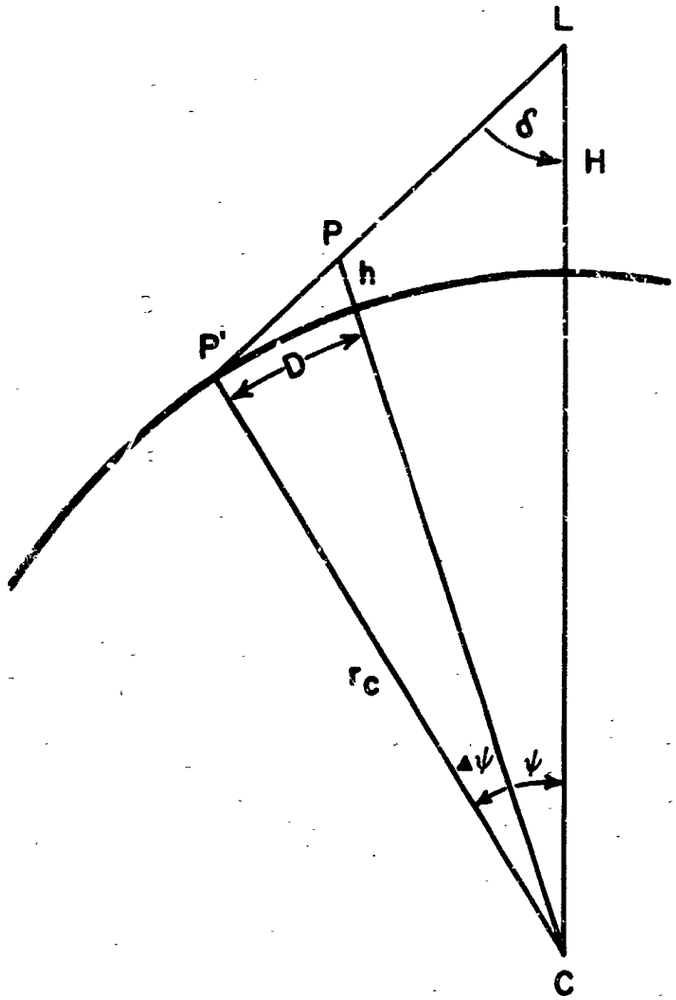

Figure 4.5: True Relief Displacement

With four variables, Eq. (4.26) is not amenable to simple graphical representation; however, a close approximation of the relief displacement can be found as shown in Fig. 4.6. The curvature of the Earth is very slight in triangle PP'Q and is neglected. Consequently,

$$D = h \tan(\psi + \delta) \quad . \tag{4.27}$$

Now ψ is a function of δ, that is,

$$\psi = \sin^{-1}\left[\frac{(r_c + H)\sin\delta}{r_c + h}\right] - \delta$$

thus Eq. (4.27) becomes

$$D = h \tan\left\{\sin^{-1}\left[\frac{(r_c + H)\sin\delta}{r_c + h}\right]\right\} \quad . \tag{4.28}$$

In the arcsine term of Eq. (4.28), h is very small compared to r_c; therefore, it can be neglected, and D becomes directly proportional to h times the tangent of the angle in brackets. Therefore, in Fig. 4.7, the displacement in km is plotted as a function of the altitude, H, of the camera station, and the angle δ, which is obtained directly from the photograph. The elevation of the object, h, is considered 1 km and r_c is taken as 6370 km. To obtain values of D corresponding to elevations other than 1 km, h is multiplied by the ordinate value of the graph.

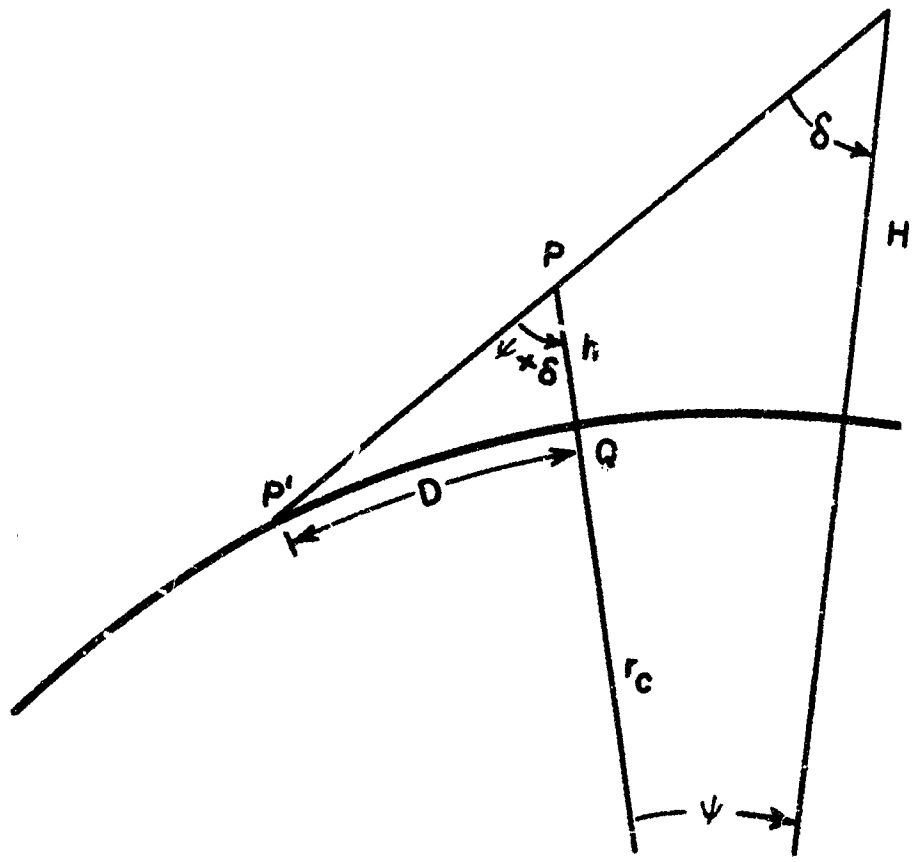

Figure 4.6: Approximate Relier Displacement

LOCKHEED
CALIFORNIA COMPANY

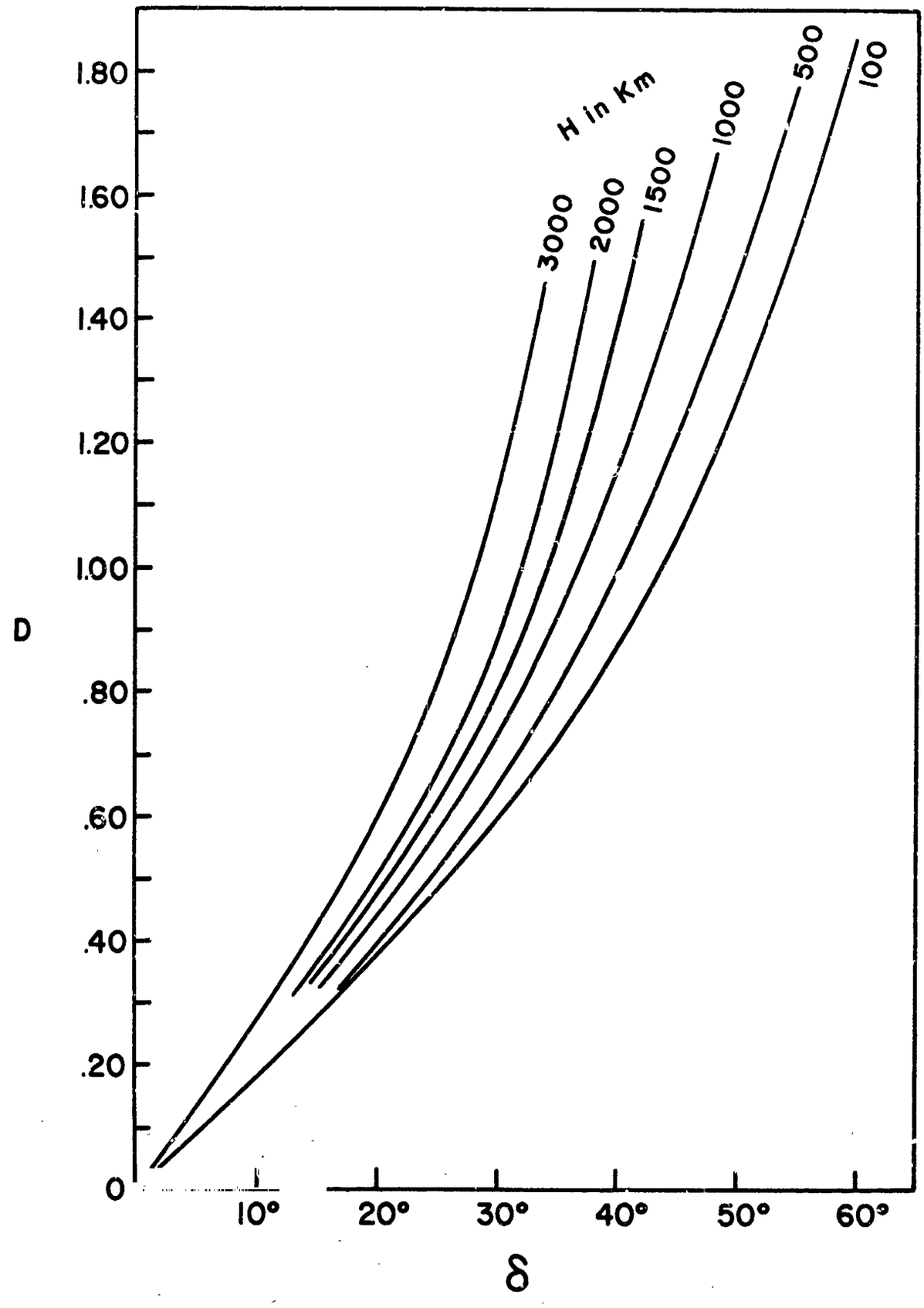

Figure 4.7: Relief Displacement for h = 1 km

Finally, the corrected values of X and Y are obtained by subtracting the components of the radial displacement (ΔX and ΔY) from X and Y, where

$$\Delta X = D \cos\left[\tan^{-1}\left[\frac{Y}{X}\right]\right] \tag{4.29}$$

$$\Delta Y = D \sin\left[\tan^{-1}\left[\frac{Y}{X}\right]\right] . \tag{4.30}$$

Hyperaltitude photography will be useful in exploring poorly known areas; consequently, elevation control will be sparse. Without such control, measurements near the horizon should be avoided because relief displacement increases rapidly with the angle to the vertical (δ).

In some cases, it may be possible to estimate the relief from the configuration of the topography in plan view. With regard to the Earth, the oceans furnish the necessary datum. Coastal plains may extend tens to hundreds of miles inland, maintaining a fairly constant slope of about $0^{\circ}01'$. Using this value, the elevation at any point on a coastal plain can be estimated. Coastal plains are best recognized by their drainage pattern. The river courses are generally very persistent in direction, which is essentially perpendicular to the coastline. Meandering is a common characteristic of coastal plain rivers.

Large river valleys such as the Amazon and Po also maintain a rather uniform gradient of about $0^{\circ}01'$. These rivers are recognized by their great length, broad flood plains, and meandering courses.

Cumulus clouds commonly hug the crests of lofty ranges, hence the presence of persistent linear cloud formations infers an elevation of several thousand feet.

In some areas tone is closely related to elevation. This is true in the Basin and Range Province of the U.S. The ranges are darker than the intermontane basins. This is due principally to three reasons: 1) the higher elevations support more vegetation, in many cases dense forest cover, 2) shadows are trapped in the rugged highlands by the craggy outcrops, trees and shrubs, 3) the freshly exposed bedrock of the ranges is darker in color owing to a greater percentage of ferromagnesium minerals.

Many plant forms are sensitively controlled by altitude for a given latitude - knowledge of this control therefore furnishes an indication of altitude. Tree lines are uniform over large geographical areas and can be exceptionally useful altitude fixes if known for the region in question.

IV-D: IMAGE DISPLACEMENT BY ATMOSPHERIC REFRACTION

Introduction

A ray of light entering a camera in space is refracted in its path through the Earth's atmosphere.* The Earth's atmosphere is non-uniform, being composed of complex strata varying in density, molecular composition, and temperature. Variations in the index of refraction accompany the changes in physical properties from one stratum to another. In general, however, a ray of light from the Earth follows a convex-upward path which is steeper near the surface of the Earth. Most of the refraction takes place in the lower, denser part of the atmosphere. Hyperaltitude photography is therefore essentially affected by the entire atmosphere.

This present work represents an alternate and simpler approach than that found in Crowson (1962), and is believed to be an improvement over the work of Munick (1962), and Merifield (1963).

Analysis

Figure 4.8 shows how refraction affects the location of an object on the Earth's surface. A light ray originating at an object P

---

* Other planetary atmospheres are not considered here owing to our lack of knowledge of their constitution.

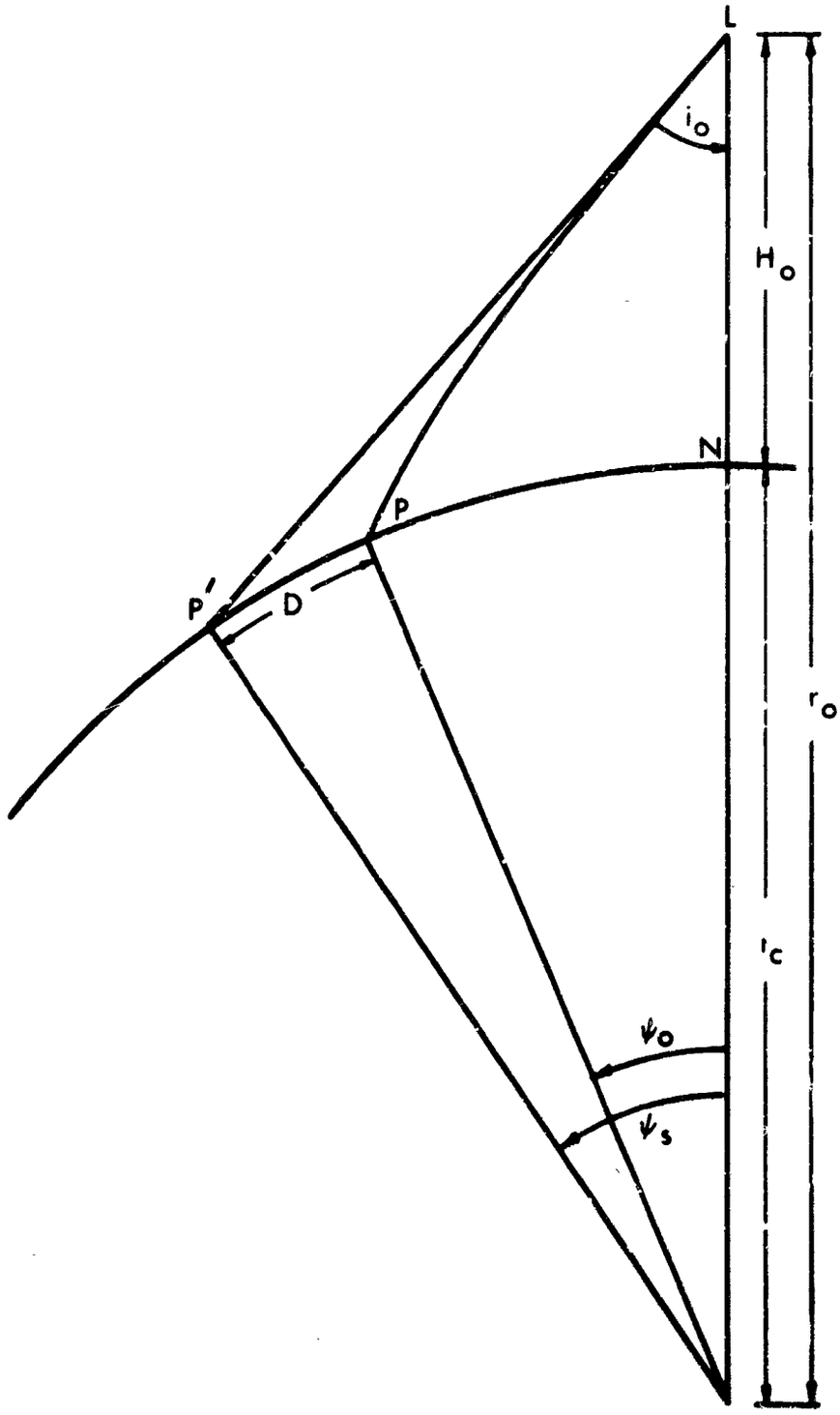

Figure 4.8: Geometry of Refraction Displacement

will follow a curved path similar to that shown in the figure. To the camera at L, the object appears to be at P', displaced a distance D from its true position. The displacement is always outward from the local ground nadir at N.

To find the true path of the ray, it would be necessary to know the index of refraction at a large number of points above the surface. There is no simple relation between the index of refraction and altitude, but as a good approximation the index of refraction may be considered to be proportional to the density. According to Eq.(4.31) density is assumed to vary as an exponential function of the altitude H:

$$\rho = \rho_o e^{-kH} \tag{4.31}$$

where ρ is the density at height H and ρ_o is the density at sea level. Equation (4.31) can be written

$$H = -\frac{1}{k} \ell n \frac{\rho}{\rho_o}$$

then

$$dH = -\frac{1}{k} d\ell n \frac{\rho}{\rho_o}$$

or

$$k = -\frac{d\ell n \frac{\rho}{\rho_o}}{dH} \quad . \tag{4.32}$$

Hence, k is the negative of the slope of the curve $\ell n \frac{\rho}{\rho_o}$ vs. H.

IV-C: RELIEF DISPLACEMENT*

The geographic location of an object is its position projected along a radius onto the reference spheroid. If the reference spheroid possessed no relief, then every object would be viewed in its true location, regardless of the perspective. In the case of the Earth, relief features of the continental areas generally lie above sea level and are not viewed in their true location except from directly overhead.

The following procedure assumes that the coordinates of the object have been determined relative to a spherical Earth, and that a correction is desired to account for relief displacement. The coordinates of the object are referred to a coordinate system whose origin is the exposure station. The Z axis is vertical and the Y axis lies in the principal plane. It is further assumed that the elevation of the object, h, is known or has been estimated.

The angle δ, which is the vertical angle between the ray from the object and the plumb line to the exposure station, is found as shown in Fig. 4.4

$$\delta = \tan^{-1}\left[\frac{\sqrt{X^2 + Y^2}}{Z}\right] . \qquad (4.22)$$

---

* Reprinted from Merifield (1963).

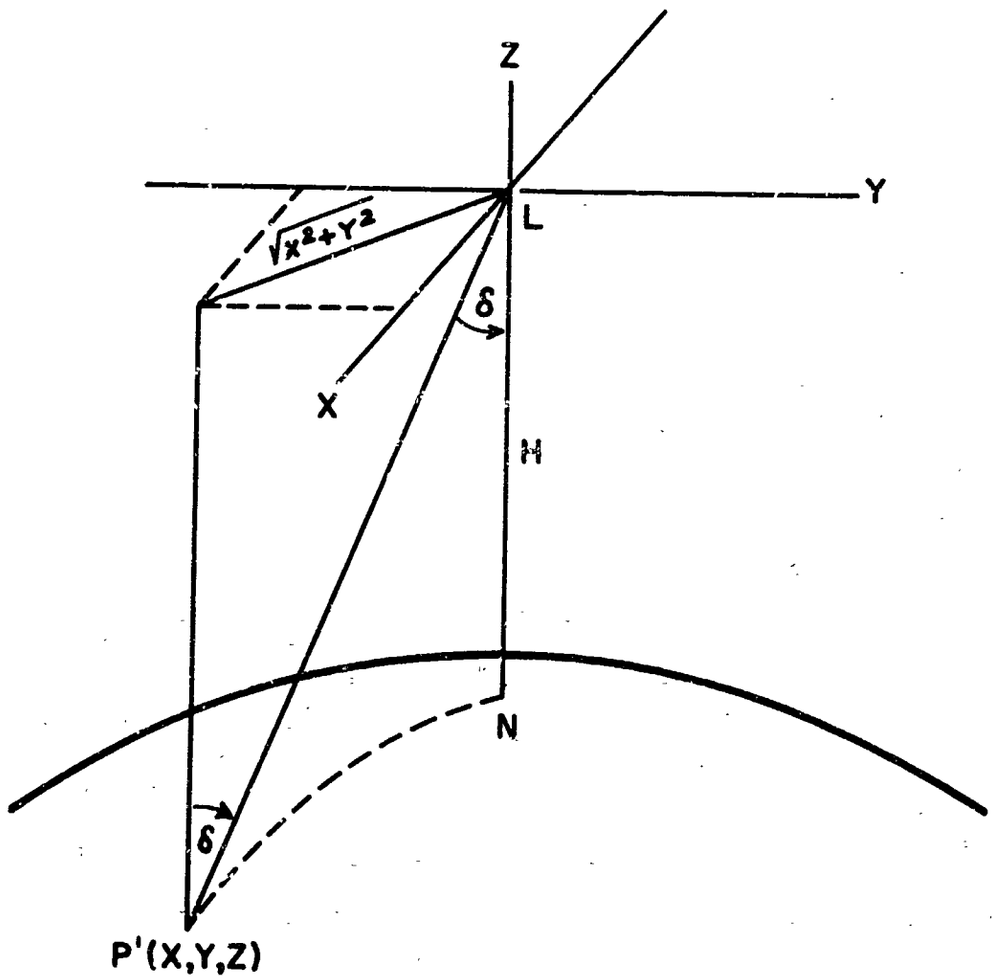

Figure 4.4: Coordinates of a Point on the Terrestrial Sphere

The reciprocal of Eq. (4.32) is known in atmospheric studies as the scale height H_s, given by

$$H_s = \frac{RT}{gM}$$

where R is the universal gas constant, T the absolute temperature, g the acceleration of gravity, and M the mean molecular weight of the atmospheric molecules. Scale height therefore depends on the acceleration of gravity, molecular weight, and temperature - all of which vary with altitude. Since 99 percent of the atmosphere lies below the altitude of 100,000 feet, most of the refraction takes place in this region. Following the assumption that the index of refraction is proportional to density, a value for the scale height weighted by the density was determined for the region below 100,000 feet. For each 5000-foot interval, the medial values for the density and scale height were chosen from the tables of the ARDC Model Atmosphere (Minzner et al, 1959). For example, for the interval between 15,000 feet and 20,000 feet, the values of ρ and H_s given for 17,500 feet were used. This is believed justified, since for intervals as small as 5000 feet, the relations are nearly linear. The weighted average $\bar{H}_s$ was then calculated from

$$\bar{H}_s = \frac{\sum \rho_i H_{s_i}}{\sum \rho_i} ,$$

yielding a value of 24.03×10^3 feet, whence

$$k = \frac{1}{H_s} = 4.16 \times 10^{-5} \text{ feet}^{-1}$$

With these assumptions, the index of refraction as a function of H can be expressed as

$$\mu - 1 = (\mu_s - 1)e^{-kH} \qquad (4.33)$$

where μ_s is the index of refraction at $H = 0$, and is equal to 1.00029 (Handbook of Chemistry and Physics). The "ones" enter into this equation because at $H = 0$, $\mu = \mu_s$ and as $H \longrightarrow \infty$, $\mu \longrightarrow 1$.

If the atmosphere is considered to be composed of a series of concentric shells, the relationship of the angles of refraction between successive layers is given by the law of refraction for spherical surfaces,

$$r_o \mu_o \sin i_o = r_i \mu_i \sin i_i \quad , \qquad (4.34)$$

where

r_o = the distance from the center of the Earth to the camera
= $r_c + H_o$

μ_o = the index of refraction at the camera
= unity at satellite altitudes

i_o = the angle between the vertical and the ray entering the camera

Accordingly, r_i, μ_i and i_i are the radial distance, index of refraction, and angle of the light ray to the vertical for the i^{th} layer of the atmosphere. Expressing the index of refraction as a function of r, the quantity $r\,\mu(r)\sin i$ remains constant along the ray of light. Thus we have

$$\sin i = \frac{r_o \mu_o \sin i_o}{r\,\mu} \quad . \tag{4.35}$$

The "slope" of the curve $r = r(\psi)$ in polar coordinates (see Fig. 4.9) is

$$\tan \alpha = \frac{1}{r}\frac{dr}{d\psi} \quad . \tag{4.36}$$

If the curve $r(\psi)$ is the path of the light ray, then

$$\alpha = 90 - i$$

and

$$\tan \alpha = \cot i \quad .$$

But

$$\cot i = (\sin^{-2} i - 1)^{\frac{1}{2}} \quad ,$$

hence, from Eqs. (4.35) and (4.36)

$$\frac{1}{r}\frac{dr}{d\psi} = \left[\left(\frac{r\,\mu}{r_o \mu_o \sin i_o}\right)^2 - 1\right]^{\frac{1}{2}} \quad . \tag{4.37}$$

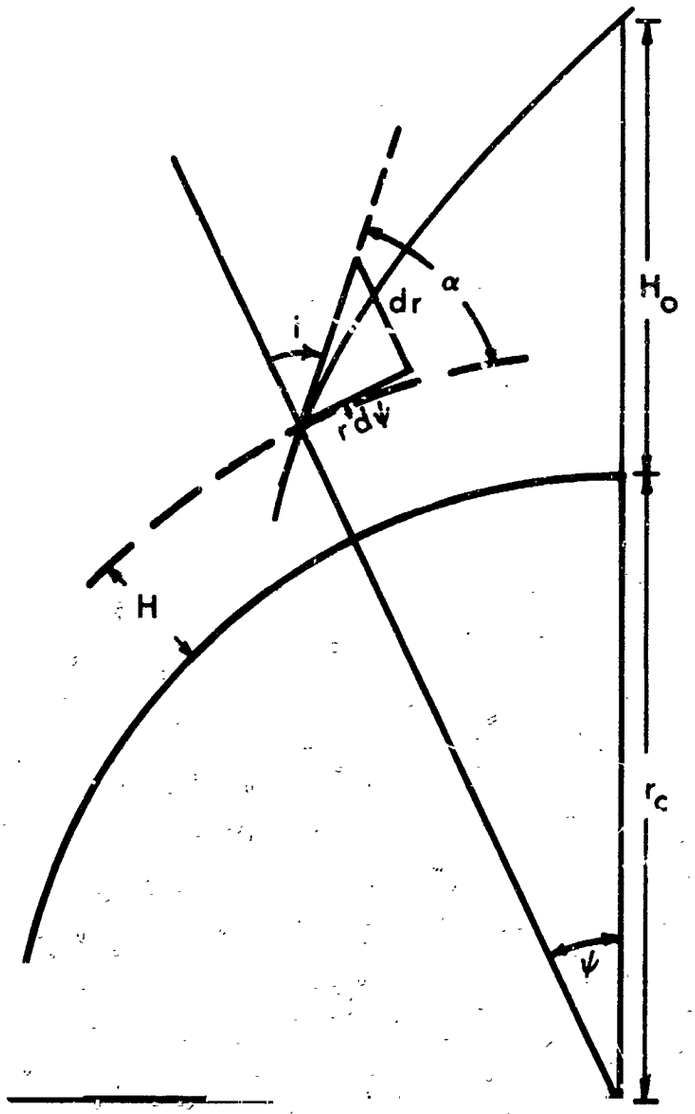

Figure 4.9: Slope of Light Ray

Separating variables, the polar angle ψ_o at which the light ray emanating at $r_o = r_c + H_o$ intersects the Earth's surface $(r = r_c)$ is obtained by integration:

$$\psi_o = \int_{r_c+H_o}^{r_c} \frac{dr}{r\left[\left(\frac{r\mu(r)}{r_o\mu_o \sin i_c}\right)^2 - 1\right]^{\frac{1}{2}}} \quad . \tag{4.38}$$

On the other hand, the direct rectilinear ray at angle i_o intersects the Earth's surface at an angle ψ_s given by

$$\psi_s = \sin^{-1}\left[\frac{r_c + H_o}{r_c} \sin i_o\right] - i_o \tag{4.39}$$

and the desired distance can be found by integrating Eq. (4.38) numerically and subtracting it from ψ_s in Eq. (4.39).

With $\mu(r)$ and μ_o differing only slightly, the difference $(\psi_s - \psi_o)$ is the difference of two large quantities, which is disadvantageous from the point of view of computation. This can be circumvented by observing that ψ_s is the identical integral Eq. (4.38) for $\mu = \mu_o$, since for μ_o = constant, the light ray is a straight line. Hence, the desired quantity is

$$\psi_s - \psi_o = \int_{r_c}^{r_c+H_o} \left\{ \left[\left(\frac{r\mu(r)}{r_o \mu_o \sin i_o} \right)^2 - 1 \right]^{-\frac{1}{2}} - \left[\left(\frac{r}{r_o \sin i_o} \right)^2 - 1 \right]^{-\frac{1}{2}} \right\} \frac{dr}{r} \quad . \tag{4.40}$$

Since $\mu(r)$ and μ_o differ only slightly, the square root is developed to the first power in $(\mu - \mu_o)$ and Eq. (4.40) becomes

$$\psi_s - \psi_o = \frac{1}{\mu_o r_o^2 \sin^2 i_o} \int_{r_c}^{r_c+H_o} \frac{r[\mu(r) - \mu_o]dr}{\left[\left(\frac{r}{r_o \sin i_o} \right)^2 - 1 \right]^{\frac{3}{2}}} \quad . \tag{4.41}$$

An exponential law for $\mu(r)$ is adopted, Eq. (4.33), and μ_o is taken as unity. Furthermore, the dimensionless height $h = \frac{H}{r_c}$ is introduced; then $r = r_c(1 + h)$, and Eq. (4.41) becomes

$$\psi_s - \psi_o = \frac{(\mu_s - 1)}{(1 + h_o)^2 \sin^2 i_o} \int_o^{h_o} \frac{(1 + h)e^{-k r_c h}}{\left\{ \left[\frac{1 + h}{(1 + h_o)\sin i_o} \right]^2 - 1 \right\}^{\frac{3}{2}}} dh \quad . \tag{4.42}$$

The important contributions to the integral stem from heights where the density is large, i.e., close to the Earth's surface. Consequently, good accuracy is obtained by developing the three-halves root in Eq. (4.42) to the first power in h as long as i_o is not close to 90°;

Eq. (4.42) then becomes

$$\psi_s - \psi_o = \frac{(\mu_s - 1)(1+h_o)\sin i_o}{\cos^3 i_o} \int_o^{h_c} (1+h) e^{-k r_c h} \left(1 + 3h_o \tan^2 i_o - \frac{3h}{\cos^2 i_o}\right) dh \, .$$

(4.43)

The integral is of the form $\int x e^{ax} dx$, which can be evaluated in closed form. In general the altitude of the camera (H_o) is large compared to the scale height (H_s) and the exponentials e^{-H_o/H_s} are then negligible; the distance of image displacement D is then

$$D = r_c(\psi_s - \psi_o) = \frac{(\mu_s - 1)(1+h_o)\sin i_o}{k \cos^3 i_o} \left[1 + 3h_o \tan^2 i_o - \frac{2 + 3(1-h_o)\tan^2 i_o}{k r_c}\right] .$$

(4.44)

For example, for H_o - 100 miles and $i_o = 60^\circ$, the displacement D is approximately 61 feet. Examination of the formula shows that the displacement becomes large only when i_o is large. But in measurements with oblique photographs, points making an angle of greater than 60° with the vertical from the camera station are not of interest because these points are near the horizon and are not readily identifiable owing to foreshortening and atmospheric haze. In general, it can be said that for the precision with which we are concerned (1-2 km), atmospheric refraction may be neglected.

REFERENCES

1. Crowson, H. L. (1962) "Effect of Atmospheric Refraction on Electromagnetic Propagation," American Rocket Society Journal, vol. 32, pp. 440-442.

2. Escobal, P. R. (1962) "An Optimum Solution to the Station Fly-Over Problem," Lockheed-California Co., LTM 50285.

3. Escobal, P. R. (1963) "Intersectron (A Machine Subroutine for the Calculation of Ground Traces)" Lockheed-California Co., LTM 50407.

4. Katz, A. H. (1950) "Contributions to the Theory and Mechanics of Photo Interpretation from Vertical and Oblique Photographs," Photogrammetric Engineering, vol. XVI, pp. 339-386.

5. Lane, B. B. (1950) "Scales of Oblique Photographs," Photogrammetric Engineering, vol. XVI, pp. 409-414.

6. Lehman, E. H., Jr. (1963) "Determining Exposure Point, Tilt, and Direction of Photograph From Three Known Ground Points," Photogrammetric Engineering, vol. XXIX, pp. 702-708.

7. Manual of Photogrammetry (1952), American Society of Photogrammetry.

8. Merifield, Paul M. (1963) "Geologic Information From Hyperaltitude Photography," Ph.D. Dissertation, University of Colorado.

9. Minzner, R. A. et al (1959) "The RADC Model Atmosphere," AFCRC-TR-59-267.

10. Moffitt, F. H. (1959) Photogrammetry, International Textbook Co., Scranton, Pa.

11. Minick, R. J. (1962) "Atmospheric Refraction as Seen from Space," American Rocket Society Journal, vol. 32, pp. 1731-1733.

12. Westinghouse Electric Corporation, Report under NAS-5-2755, Job Order No. 671R67-07 (1963).

APPENDIX

COMPUTER PROGRAM OF

THE LEHMAN METHOD

SUMMARY FLOW DIAGRAM OF THE LEHMAN METHOD OF PHOTOGRAPHIC ORIENTATION

Given:

pl = Effective focal length, (corrected for print enlargement)

I_α = Space coordinates of three ground control points (I = A, B, C; α = x, y, z, the origin is at A, the lowest of the three objects, and +x points east with +y pointing north.)

ij = Distances between the three control points on the photo, (i, j = a, b, c).

ip = Distances between the three control points and the principal point of the photo.

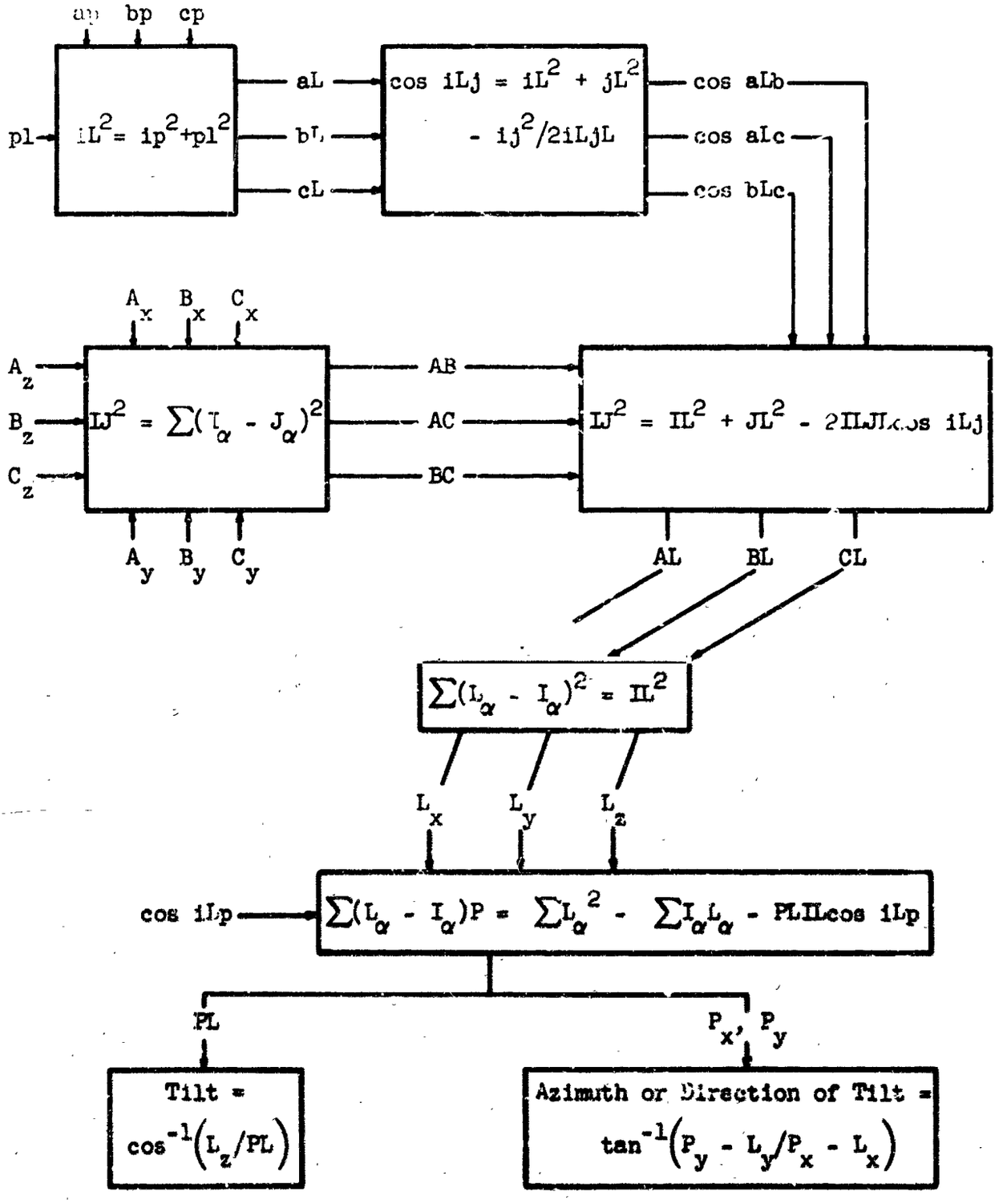
ap bp cp
pl
$iL^2 = ip^2 + pl^2$
aL
bL
cL
$\cos iLj = iL^2 + jL^2 - ij^2/2iLjL$
cos aLb
cos aLc
cos bLc
A_x B_x C_x
A_z
B_z
C_z
$LJ^2 = \sum(I_\alpha - J_\alpha)^2$
A_y B_y C_y
AB
AC
BC
$LJ^2 = IL^2 + JL^2 - 2ILJL\cos iLj$
AL BL CL
$\sum(L_\alpha - I_\alpha)^2 = IL^2$
L_x L_y L_z
cos iLp
$\sum(L_\alpha - I_\alpha)P = \sum L_\alpha^2 - \sum I_\alpha L_\alpha - PLILcos\ iLp$
PL
P_x, P_y
Tilt = $\cos^{-1}(L_z/PL)$
Azimuth or Direction of Tilt = $\tan^{-1}(P_y - L_y/P_x - L_x)$

INPUT 0.4701000E-03 0. 0. 0. 0.1290000E 02 -0.1705000E 02
0. -0.2180000E 02 -0.1410000E 02 -0.8000000E-01 0.4540000E-04 0.5960000E-04 0.7880000E-04
0.4560000E-04 0.5730000E-04 0.2170000E-04 0.

EXPOSURE POINT COORDINATES -0.2356395E 02 0.6921927E 02 0.1872292E 03

GROUND NADIR N = (-0.2356395E 02 , 0.6921927E 02 , 0.)

TILT = 0.2465959E 02 COS TILT = 0.9048827E 00

PHI = -0.3258332E 02TAN PHI = -0.7682062E 01

PRINT OUT EXPLANATION

Input (km) pL A_x A_y A_z B_x B_y

B_z C_x C_y C_z ab ac bc

ap bp cp

(Output)

Exposure Point Coordinates L_x L_y L_z

Ground Nadir N = (N_x N_y N_z)

Tilt = (degrees)

PHI = (degrees) Angle between the
+ x axis and the projection of
the principal line upon the plane
z = 0

```
C     PHOTO DETERMINATIONS
      DIMENSION A(3),B(3),C(3),XL(3),P(3)
    8 READ (5,100) PL,A,B,C,SAB,SAC,SBC,SAP,SBP,CP                    ,1    ,2    ,3
      READ (5,100) AL                                                 ,4    ,5    ,6
  100 FORMAT (8F9.0)
      DELV =-.025                                                     ,7
      IF (PL) 1000,1000,9                                             ,8
    9 AB2= (A(1)-B(1))**2 + (A(2)-B(2))**2 + (A(3)-B(3))**2           ,9
      WRITE (6,901) PL,A,B,C,SAB,SAC,SBC,SAP,SBP, CP  ,AL             ,10   ,11   ,12
  901 FORMAT ( 6H1INPUT6E17.7/7E17.7/7E17.7)
      BC2= (B(1)-C(1))**2 + (B(2)-C(2))**2 + (B(3)-C(3))**2           ,13
      AC2= (A(1)-C(1))**2 + (A(2)-C(2))**2 + (A(3)-C(3))**2           ,14
      SAL2= SAP**2 + PL**2                                            ,15
      SBL2= SBP**2 + PL**2                                            ,16
      SCL2= SCP**2 + PL**2                                            ,17
      CSALB= (SAL2 + SBL2 -SAB**2)/(2.*SQRT(SAL2)*SQRT(SBL2))         ,18
      CSBLC= (SBL2 + SCL2 -SBC**2)/(2.*SQRT(SBL2)*SQRT(SCL2))         ,19
      CSALC= (SAL2 + SCL2 -SAC**2)/(2.*SQRT(SAL2)*SQRT(SCL2))         ,20
      IF (AL) 40,40,16                                                ,21
   40 C1= AB2/(1.-CSALB**2)                                           ,22
      C2= AC2/(1.-CSALC**2)                                           ,23
      IF (SQRT(C1)-SQRT(C2)) 20,20,21                                 ,24
   20 AL= SQRT(C1)                                                    ,25
      GO TO 16                                                        ,26
   21 AL=  SQRT(C2)                                                   ,27
   16 LZ=0                                                            ,28
  161 NOW=1                                                           ,29
   13 F= (CSALB**2 + CSALC**2 -CSALB*CSALC*CSBLC -1.)* AL**2 +((CSALB-
     1CSALC*CSBLC)* SQRT(AB2 -AL**2*(1.-CSALB**2))) *AL - CSBLC* SQRT(AB1723015
     22- AL**2*(1.- CSALB**2))*SQRT(AC2 -AL**2*(1.-CSALC**2)) + .5*(AB2
     3+AC2 -BC2)+(CSALC-CSALB*CSBLC)*SQRT(AC2-AL**2*(1.-CSALC**2))*AL ,30
      GO TO (131,132     ),NOW                                        ,31
  131 F1=F                                                            ,32
      AL1=AL                                                          ,33
      DAL = AL*DELV                                                   ,34
      AL=AL+DAL                                                       ,35
      NOW = 2                                                         ,36
      GO TO 13                                                        ,37
  132 LZ=LZ+1                                                         ,38
      IF (LZ-30) 10,11,10                                             ,39
   11 WRITE (6,101)                                                   ,40   ,41
  101 FORMAT (17HOITERATION FAILED)
      GO TO 8                                                         ,42
   10 FP= (F-F1)/DAL                                                  ,43
      AL= AL1 - F1/FP                                                 ,44
      IF (ABS (AL-AL1)- .0005)   12,12,161                            ,45
   12 IF (AL) 14,14,15                                                ,46
   14 WRITE (6,105) AL                                                ,47   ,48   ,49
  105 FORMAT  (19HONEGATIVE ROOT, AL=E17.7)
      GO TO 8                                                         ,50
   15 BL= AL* CSALB + SQRT(AB2 - AL**2*(1.-CSALB**2))                 ,51
      CL= AL* CSALC + SQRT(AC2 - AL**2*(1.-CSALC**2))                 ,52
      IF (BL) 17,17,18                                                ,53
   18 IF (CL) 17,17,19                                                ,54
   17 WRITE (6,102)                                                   ,55   ,56
```

```
      EXTERNAL FORMULA NUMBER  -  SOURCE STATEMENT  -  INTERNAL FORMULA NUMBER(S)

  102 FORMAT (18HONEGATIVE DISTANCE)
      GO TO 8                                                                    ,57
   19 A1=-B(3)*CL**2 +C(3)*CL**2-C(3)*B(1)**2 +B(3)*C(1)**2 - C(3)*B(2)
     1**2 +B(3)*C(2)**2 -C(3)*B(3)**2 +B(3)*C(3)**2+B(3)*AL**2-C(3)*AL**
     32                                                                          ,58
      A2= -2.*(B(3)*C(1)-B(1)*C(3))                                              ,59
      A3=  2.*(B(3)*C(2)-C(3)*B(2))                                              ,60
      A4= CL**2*B(2) - BL**2*C(2) - AL**2*B(2) +AL**2*C(2) - C(1)**2*B(2
     1) + B(1)**2*C(2) - C(2)**2*B(2) + B(2)**2*C(2) -C(3)**2*B(2) +
     2 B(3)**2*C(2)                                                              ,61
      A5= 2. *(B(2)*C(1) - B(1)*C(2))                                            ,62
      A6= 2.* B(3)*C(2) - 2.*C(3)*B(2)                                           ,63
      A7= 1. + (A2/A3)**2 + (A5/A6)**2                                           ,64
      A8= 2.*(A1*A2/A3**2 + A4*A5/A6**2)                                         ,65
      A9=(A1/A3)**2 + (A4/A6)**2  -AL**2                                         ,66
      X1= (-A8 + SQRT(A8**2 - 4.*A7*A9))/(2.*A7)                                 ,67
      X2= (-A8 - SQRT(A8**2 - 4.*A7*A9))/(2.*A7)                                 ,68
      XL(3)=(A4+ A5*X1)/A6                                                       ,69
      IF(XL(3)) 24,24,25                                                         ,70
   24 XL(3)= (A4 + A5*X2)/A6                                                     ,71
      IF (XL(3)) 27,28,28                                                        ,72
   27 WRITE (6,206) XL(3)                                                        ,73   ,74   ,75
  206 FORMAT ( 1H0,E17.7,3X37HBOTH ROOTS GIVE NEGATIVE Z-COORDINATE)
      GO TO 8                                                                    ,76
   28 XL(2)= (A1 + A2*X2)/A3                                                     ,77
      XL(1)=X2                                                                   ,78
      GO TO 26                                                                   ,79
   25 XL(2)= (A1 + A2*X1)/A3                                                     ,80
      XL(1) =X1                                                                  ,81
   26 CSALP= (SAL2   +PL**2 -SAP**2)/(2.* PL* SQRT(SAL2))                        ,82
      CSBLP= (SBL2   +PL**2 -SBP**2)/(2.* PL* SQRT(SBL2))                        ,83
      CSCLP= (SCL2   +PL**2 -SCP**2)/(2.* PL* SQRT(SCL2))                        ,84
      D=(XL(1)* B(2)* C(3) +XL(2)* B(3)* C(1) +XL(3)* B(1)* C(2))-
     1   (C(1)* B(2)*XL(3) + C(2)* B(3)*XL(1) + C(3)* B(1)*XL(2))               ,85
      B1=+1./D     *((AL*CSALP*(XL(2)-B(2)) * (XL(3)-C(3)) + (XL(2) - A(2
     1))*(XL(3)-B(3))* CL*CSCLP  +(XL(3)-A(3)) * BL*CSBLP*(XL(2)-C(2)))
     2-(CL*CSCLP *(XL(2)-B(2)) *(XL(3)-A(3)) +((XL(2)-C(2))*(XL(3)-B(3))
     3* AL*CSALP) +(XL(3)-C(3))* BL*CSBLP *(XL(2)-A(2))))                       ,86
      B2= +1./D          *(((XL(1)-A(1))* BL*CSBLP*(XL(3)-C(3)) + AL*CSAL
     1P*(XL(3)-B(3))*(XL(1)-C(1)) +(XL(3)-A(3))*(XL(1)-B(1))* CL*CSCLP)
     2- ((XL(1)-C(1))* BL*CSBLP*(XL(3)-A(3)) + CL*CSCLP*(XL(3)-B(3))*
     3(XL(1)-A(1)) + (XL(3)-C(3)) * (XL(1)-B(1)) * AL * CSALP))                 ,87
      CPL=XL(3)/SQRT(1.-B1**2-B2**2)                                             ,88
      P(1) = XL(1)- CPL*(+B1)                                                    ,89
      P(2)=XL(2)-CPL*(+B2)                                                       ,90
      P(3)=0.                                                                    ,91
      CTILT =XL(3)/CPL                                                           ,92
      TILT = ACOS(CTILT)   *57.2957795                                           ,93
    5 TPHI = (P(2) - XL(2))/(P(1) -  XL(1))                                      ,94
      PHI = ATAN(TPHI) *57.2957795                                               ,95
      WRITE (6,103)XL,XL(1),XL(2), TILT,CTILT,PHI,TPHI                           ,96   ,97   ,98
  103 FORMAT (29HOEXPOSURE POINT COORDINATES  3E17.7/1HO20HGROUND NADIR
     1 N =  (E15.7,2H ,E17.7,6H , 0.)/1HO,7HTILT = E17.7,3X11HCOS TILT =
     2 E17.7/
     21HO6HPHI = E17.7,10HTAN PHI = E17.7)
      GO TO 8                                                                    ,99
```

```
1000 STOP                                              ,100
     END                                               9977,101
```